Am J Cancer Res 2026;16(11):4794-4814
www.ajcr.us /ISSN:2156-6976/ajcr0173807

Original Article

ETV5 inhibits the proliferation of lung adenocarcinoma cells by upregulating FOXA2 expression

Ming Gong[1*], Xingshu Zhang[2*], Hao Li[3]

[1]Department of Thoracic Surgery, The Affiliated Hospital of Zunyi Medical University, Zunyi 563000, Guizhou, China; [2]Department of Thoracic Surgery, First Affiliated Hospital of Guizhou University of Traditional Medicine, Guiyang 550001, Guizhou, China; [3]Department of Oncology, Guiyang Public Health Clinical Center, Guiyang 550033, Guizhou, China. [*]Equal contributors.

Received May 6, 2026; Accepted October 25, 2026; Epub November 15, 2026; Published November 30, 2026

Abstract: Lung adenocarcinoma (LUAD) is a major subtype of lung cancer, but the roles of E26 transformation-specific variant (ETV) family members in LUAD are still not fully understood. In this study, we examined ETV1, ETV4, and ETV5 using transcriptomic, methylation, single-nucleotide variation (SNV), and copy number variation data from The Cancer Genome Atlas (TCGA). Single-cell and spatial transcriptomic data were also included in the analysis. The findings were further examined in independent Gene Expression Omnibus (GEO) cohorts and by functional experiments. ETV1 and ETV5 showed lower expression in LUAD tumors, whereas ETV4 showed higher expression. Higher ETV expression was also associated with better survival. Among these genes, ETV5 showed an independent association with favorable prognosis in multivariable Cox analysis. ETV5 overexpression reduced cell proliferation and increased apoptosis in both A549 and H1975 cells. The same growth-suppressive effect was also observed in xenograft experiments. ETV5 positively regulated forkhead box A2 (FOXA2) expression, and the expression levels of ETV5 and FOXA2 were positively correlated in an independent LUAD cohort. Luciferase assays and chromatin immunoprecipitation-quantitative polymerase chain reaction assays further supported direct transcriptional regulation of FOXA2 by ETV5. FOXA2 knockdown partially reversed the reduction in cell viability and proliferation caused by ETV5 overexpression and also reduced ETV5-induced apoptosis. These findings identify ETV5 as a tumor-suppressive transcriptional regulator in LUAD and support the ETV5-FOXA2 axis as a functionally relevant pathway with prognostic significance.

Keywords: E26 transformation-specific variant, forkhead box A2, lung adenocarcinoma

Introduction

Lung cancer is one of the most common cancers worldwide and remains a leading cause of cancer-related death [1]. In 2022, about 2.5 million people worldwide were newly diagnosed with the disease [2]. Among all lung cancer cases, more than 40% are diagnosed as adenocarcinoma [3]. Even after surgery, patients with lung adenocarcinoma (LUAD) still face a risk of tumor recurrence and metastasis [4]. A better understanding of the mechanisms involved in LUAD may help improve early diagnosis and support more precise treatment. Tobacco use is also well established as a major risk factor for lung cancer [5]. Some studies have suggested that women who smoke may have a higher risk of developing lung cancer than men who smoke. This difference may be partly related to higher pulmonary expression of cytochrome P450 family 1 subfamily A member 1 (CYP1A1) in women [6]. Long-term exposure to substances such as silica, asbestos, and beryllium is also associated with an increased risk of lung cancer [7, 8]. LUAD is highly heterogeneous at the molecular level and often carries driver alterations in genes such as epidermal growth factor receptor (EGFR), anaplastic lymphoma kinase (ALK), Kirsten rat sarcoma viral oncogene homolog (KRAS), and B-Raf proto-oncogene (BRAF), including the BRAF V600E mutation [9]. Beyond traditional molecular classifications, several molecular markers have been linked to LUAD progression. The focal adhesion kinase (FAK) pathway, for example, shows different expres-

https://doi.org/10.62347/ZSWX6913

sion patterns across stages of LUAD, and higher FAK expression is associated with more advanced disease [10]. These findings suggest that FAK may have potential as a biomarker for the early diagnosis of LUAD and may also be relevant to its clinical assessment.

The E26 transformation-specific variant (ETV) family includes ETV1, ETV4, and ETV5 and forms an important subgroup of the E26 transformation-specific (ETS) transcription factor superfamily. These proteins bind to DNA through the C-terminal ETS domain, while the N-terminal pointed domain is involved in oligomerization and transcriptional activation [11]. Under normal physiological conditions, ETV proteins play important roles in embryonic development, cell proliferation, and differentiation. Abnormal ETV expression, however, has been linked to tumor development and may promote cancer progression [12]. Studies have shown that ETV genes can be overexpressed, amplified, or translocated in different types of cancer, which may result in abnormal transcriptional activity [13]. For example, gene fusions can lead to abnormally high ETV4 expression in prostate cancer, which has been associated with disease progression [14]. In Ewing sarcoma, the Ewing sarcoma breakpoint region 1 (EWSR1)-ETV1 fusion gene can act as an important oncogenic driver [15]. ETV1 amplification has also been reported in melanoma, where it may cooperate with BRAF V600E to promote tumor progression [16]. These findings support an important role for ETV family members in cancer and suggest that they may represent potential therapeutic targets.

Our study examined the roles and possible mechanisms of ETV family members in LUAD by combining multi-omics analysis with experimental validation. We analyzed bulk RNA-seq data from TCGA to assess genetic alterations, expression patterns, and clinical associations of ETV members. Single-cell and spatial transcriptomic data were used to examine their distribution across different cell populations and tissue regions. We also constructed a core ETV regulatory network and performed functional enrichment analysis to explore possible downstream pathways. *In vitro* experiments were then used to assess how ETV5 affects lung cancer cell proliferation and apoptosis. The overall study design is shown in **Figure 1**. These analyses were intended to clarify the biological roles of ETV family members in LUAD and to evaluate their possible value as prognostic biomarkers or therapeutic targets.

Methods and materials

Data acquisition

Data for LUAD from the TCGA-LUAD cohort, encompassing transcriptome, clinical records, methylation, single-nucleotide variation (SNV), and copy number variation (CNV), were obtained from TCGA. The University of California, Santa Cruz (UCSC) Xena platform (https://xena.ucsc.edu/) was used for this purpose, which serves as an interface for the Genomic Data Commons (GDC) Data Portal (https://portal.gdc.cancer.gov/).

Analysis of ETV family and clinical pathological characteristics

We used the Wilcoxon rank-sum test to examine the associations between the molecular features of ETV family members (gene expression, methylation, CNV, and SNV), and key clinicopathological characteristics, including gender, age, and pathological stage.

Single-cell RNA-seq data analysis

We used the Seurat R package to process the single-cell RNA-seq (scRNA-seq) dataset GSE131907, which was downloaded from the Gene Expression Omnibus (GEO) database. The dataset included 11 tumor and 11 matched normal samples from patients with LUAD. The Percentage Feature Set function was used to calculate the mitochondrial and ribosomal RNA percentages. Low-quality cells were filtered out by applying thresholds: Cells must contain between 50 and 8000 expressed genes and have a mitochondrial RNA percentage < 5%. After quality control, 86,739 cells were eligible for downstream analysis. Cell types within different clusters were annotated in accordance with the annotation schema provided by the Tumor Immune Single-cell Hub database.

Spatial transcriptomics expression analysis

To study the spatial expression patterns of the ETV family, we analyzed the SCAR_ST_000010 dataset from the SCAR database (http://scaratlas.com) to visualize key gene expression.

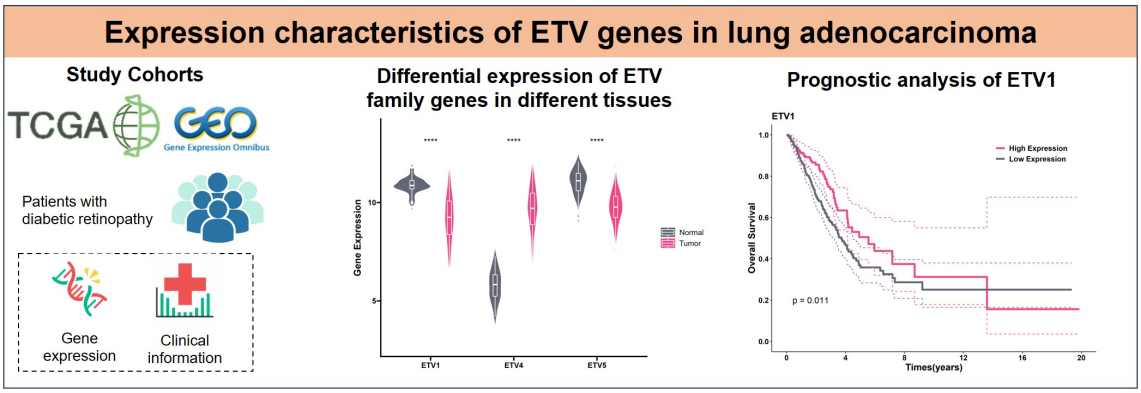
Expression characteristics of ETV genes in lung adenocarcinoma
Study Cohorts
TCGA
GEO
Gene Expression Omnibus
Patients with diabetic retinopathy
Gene expression
Clinical information
Differential expression of ETV family genes in different tissues
Gene Expression
Normal
Tumor
ETV1
ETV4
ETV5
Prognostic analysis of ETV1
ETV1
High Expression
Low Expression
Overall Survival
p = 0.011
Times(years)

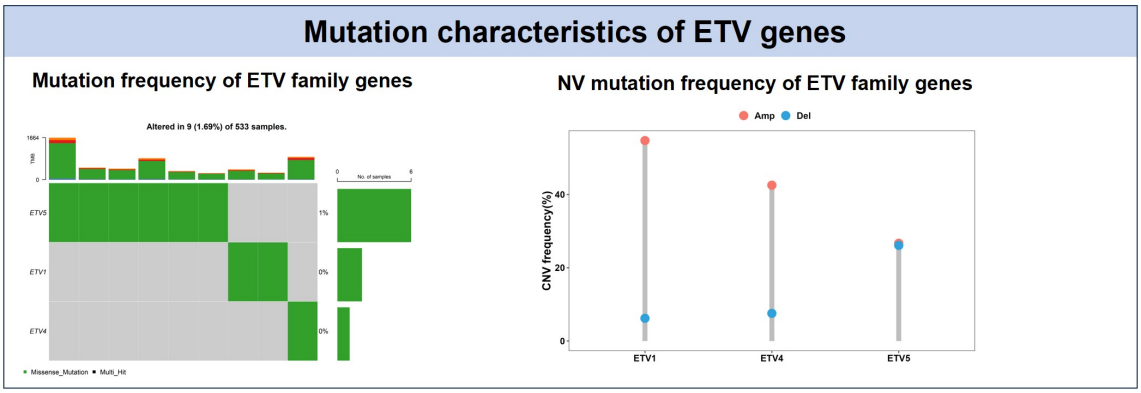
Mutation characteristics of ETV genes
Mutation frequency of ETV family genes
Altered in 9 (1.69%) of 533 samples.
ETV5
ETV1
ETV4
Missense_Mutation
Multi_Hit
NV mutation frequency of ETV family genes
Amp
Del
CNV frequency(%)
ETV1
ETV4
ETV5

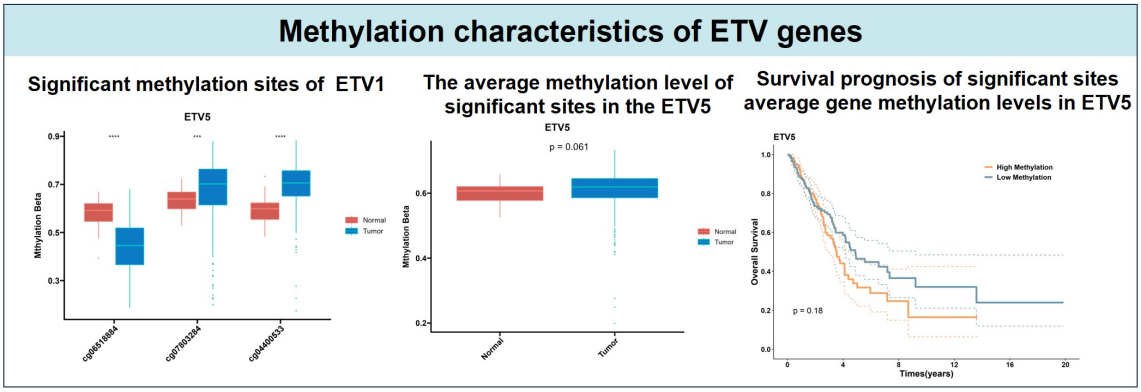
Methylation characteristics of ETV genes
Significant methylation sites of ETV1
ETV5
Mthylation Beta
Normal
Tumor
cg06516884
cg07803284
cg04400533
The average methylation level of significant sites in the ETV5
ETV5
p = 0.061
Survival prognosis of significant sites average gene methylation levels in ETV5
ETV5
High Methylation
Low Methylation
Overall Survival
p = 0.18
Times(years)

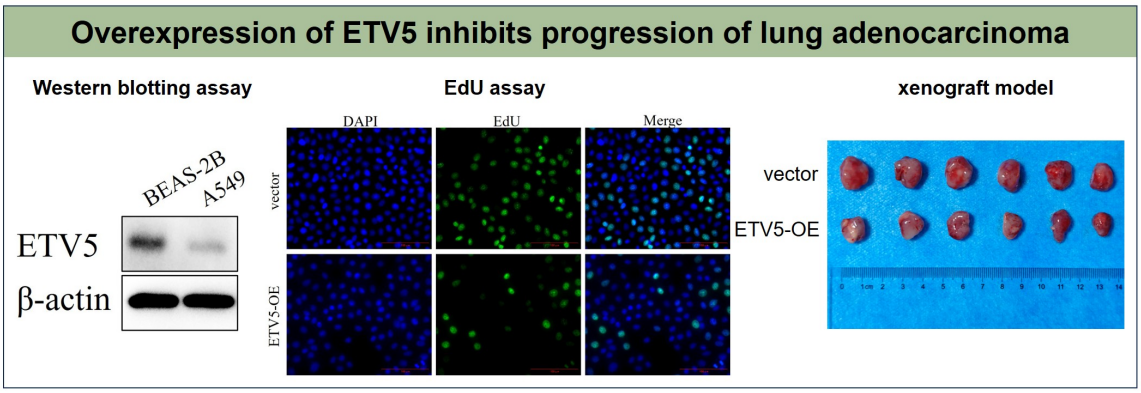
Overexpression of ETV5 inhibits progression of lung adenocarcinoma
Western blotting assay
BEAS-2B
A549
ETV5
β-actin
EdU assay
DAPI
EdU
Merge
vector
ETV5-OE
xenograft model
vector
ETV5-OE

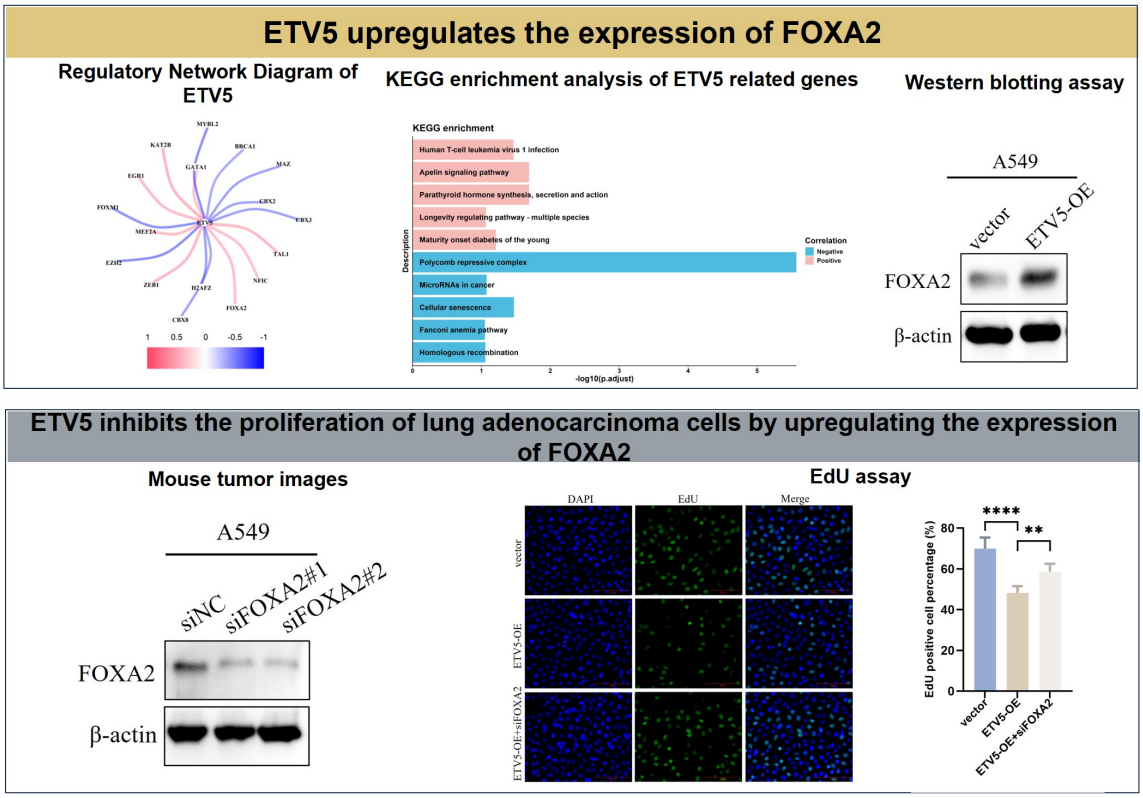

Figure 1. Flowchart of the study.

ETV family regulatory network construction

The regulatory targets of the ETV family were obtained from the Encyclopedia of DNA Elements (ENCODE) Transcription Factor Targets dataset via the Harmonizome portal. Subsequently, correlation analysis between these targets and ETV family members was performed in the TCGA-LUAD cohort to identify significantly co-expressed genes.

Functional enrichment and interaction analysis

Functional enrichment analysis, encompassing gene ontology (GO) terms and Kyoto encyclopedia of genes and genomes (KEGG) pathways, was performed on the identified gene set using the ClusterProfiler R package. Gene annotations were obtained using the org.Hs.eg.db package. Results with a false discovery rate adjusted to $P < 0.05$ were considered statistically significant.

Kaplan-Meier survival analysis

The overall survival (OS) curve was plotted using the Kaplan-Meier method, and differences between groups were compared using the two-sided log-rank test. For the mRNA expression of ETV1, ETV4, and ETV5, the optimal cutoff values for the high- and low-expression groups were determined by the surv_cutpoint function of the survminer package in R, based on the maximally selected rank statistics (maxstat), with each group containing at least 30% of the patients (minprop = 0.3). For methylation, the average β-value of the significantly differentially methylated probes (tumor versus normal, Wilcoxon test $P < 0.05$) in each sample was calculated, and the patients were divided into high- and low-methylation groups based on the median of this average β-value. CNVs and mutation analyses did not involve expression cutoff values and were grouped following the gene copy number variation status (variant versus wild-type/diploid) and somatic mutation status (mutant versus wild-type).

Multivariable cox regression analysis

Multivariable Cox proportional hazards regression analysis was performed using the GSE68465 cohort. ETV5 expression was analyzed as a continuous variable and standard-

ized per standard deviation (SD). The clinical covariates included age, sex, smoking status, T stage, and N stage. Age was modeled per 10-year increase, while categorical variables were coded as male versus female, ever-smoker versus never-smoker, T3-4 versus T1-2, and N1-2 versus N0. Hazard ratios (HRs) and corresponding 95% confidence intervals (CIs) were calculated. Variables with $P < 0.05$ were considered statistically significant.

Validation of the ETV5-Forkhead box A2 (FOXA2) correlation in an independent LUAD cohort

A correlation analysis of ETV5 and FOXA2 expression was conducted using the GSE31210 dataset from the GEO database of LUAD. This dataset contains a complete series matrix of 246 samples, including 226 primary LUAD tissues (tumor) and 20 normal lung tissues (normal). First, the expression values of ETV5 and FOXA2 in each tumor sample were extracted. After excluding samples with missing expression values for any gene, Spearman's rank correlation was performed. Finally, 226 tumor samples were included. The *P*-value of the correlation coefficient test was corrected for multiple tests using the Benjamini-Hochberg method in the entire expression correlation verification cohort. The analysis was completed in R (version 4.3.1), with data organization using data table 1.17.4, correlation tests using the cor.test function in stats 4.3.1, and result visualization using ggplot2 3.5.1 and ggpubr 0.6.0.

Correlation analysis of ETV5-specific CpG methylation probe signals with ETV5 transcriptional level

The correlation analysis of ETV5-specific CpG site methylation and transcriptional levels was conducted using the Illumina HumanMethylation450 BeadChip β-value matrix and RNA-seq transcripts-per-million (TPM) expression matrix from the TCGA-LUAD cohort. The original 450 K methylation data included 503 samples, among which 469 were primary tumors, 32 were normal tissues, and 2 were recurrent tumor samples; 469 primary tumor samples corresponded to 458 different patients. The RNA-seq matrix included 600 samples, among which 539 were primary tumors, 59 were normal tissues, and 2 were recurrent tumor samples, corresponding to 516 patients with primary tumors. The analysis only included patients whose methylation and RNA-seq data could be matched according to the TCGA patient barcodes for primary tumors. For patients with multiple primary tumor samples, the 01A sample was prioritized for retention, resulting in 455 matching patients. Normal and recurrent tumor samples were excluded from the correlation analysis. Based on the previous results of differential methylation between tumor and normal tissues, three probes, cg06518884, cg07803284, and cg04400533, were pre-specified. The ETV5 transcriptional level was converted to log2 (TPM1), and Spearman rank correlation was used as the main analysis, Pearson correlation as the sensitivity analysis, and the Benjamini-Hochberg method was used to correct *P*-values among the three pre-specified probes. Both cg06518884 and cg04400533 had 455 pairs of complete observations, while cg07803284 had 452 pairs of complete observations due to the absence of probe β values for three patients. The probe regions were annotated according to IlluminaHumanMethylation450kanno.ilmn12. hg19 0.6.1, where TSS1500, TSS200, 5'UTR, or the first exon were defined as the promoter region, and enhancers, genomic regions, CpG islands, island shores, island shelves, and open sea areas were also recorded.

Materials

Overexpression lentivirus was synthesized by GenePharma (Shanghai, China). siRNA was synthesized by Tsingke Biotechnology (Beijing, China). Opti-MEM was procured from Yuanye Bio-Technology Co., Ltd. (Shanghai, China). ETV5 Polyclonal antibody (Cat No. 13011-1-AP) and FOXA2 Polyclonal antibody (Cat No. 22474-1-AP) were bought from Proteintech (Wuhan, China). Annexin V-fluorescein isothiocyanate (FITC)/propidium iodide (PI) Apoptosis Detection Kit (40302ES20) and 488 5-ethynyl-2'-deoxyuridine (EdU) Fluorescence Imaging Assay kit (40275ES60) were bought from YEASEN (Shanghai, China). BEAS-2B cells (C6106), A549 cells (C6053), and H1975 cells (C6655) were acquired from Beyotime (Shanghai, China). ChIP-IT High Sensitivity® kit was bought from Active Motif (Cat. No. 53040).

Cell culture and lentiviral transduction/siRNA transfection

BEAS-2B and A549 cells were cultured in their respective media (Roswell Park Memorial Institute -1640 and F-12K), each containing 10% fetal bovine serum (FBS). H1975 cells were cultured in RPMI-1640 supplemented with 10% FBS. All cultures were maintained in a humidified incubator at 37°C with a 5% CO_2 supply. For gene manipulation, cells were transduced with lentiviral overexpression vectors or transfected with siRNA, following the manufacturer's protocols. Stably transduced cells were selected using the appropriate antibiotics. For FOXA2 knockdown, cells were transfected with FOXA2- siRNA or negative-control siRNA using Lipofectamine 3000 (L3000001, Thermo Fisher) according to the manufacturer's protocol. A total of 50 nM siRNA was used for each transfection. Cells were incubated for 48 h after transfection before subsequent functional and molecular analyses.

Western blotting

Following harvest, the cells were lysed in radio immunoprecipitation assay lysis buffer (RIPA) containing protease and phosphatase inhibitors. Protein concentration was quantified using a commercial assay kit, strictly adhering to the manufacturer's instructions, and samples were prepared accordingly. Proteins were separated by molecular weight via sodium dodecyl sulfate-polyacrylamide gel electrophoresis and subsequently blotted onto PVDF membranes using a standard transfer apparatus. The membranes were blocked using 5% non-fat milk. Subsequently, they were probed first with primary antibodies, including β-actin (1:5000, 66009-1-Ig, Proteintech), ETV5 (1:1000, 13011-1-AP, Proteintech), and FOXA2 (1:500, 22474-1-AP, Proteintech), overnight at 4°C, and then with appropriate horseradish peroxidase-linked secondary antibodies (1:5000, C31430100, Thermo Fisher). Subsequently, detection was performed using an enhanced chemiluminescence reagent, and the resulting signals were imaged.

Cell counting Kit-8 (CCK-8) assay

Following the designated treatments, the cells were collected, centrifuged, and counted. Cells were seeded by adding 100 μL of a cell suspension (5×10^3 cells/well) to a 96-well plate. Cells were then cultured under standard humidified conditions (37°C, 5% CO_2) for the indicated times. Subsequently, 10 μL of CCK-8 solution was added to each well, and the plate was returned to the incubator for 4 h. Signal detection was performed by measuring the absorbance at 450 nm using a microplate reader. Each experimental condition was evaluated through more than three technical repetitions in each experiment, and the entire experiment was independently repeated three times. Statistical analysis was conducted using the average values of the technical repetitions in each experiment.

EdU assay

Cells in the exponential growth phase were seeded into a 96-well plate at a density of 5×10^3 cells/well and subjected to the specified treatments. After 24 h, the culture medium was replaced with EdU working solution (10 μM), followed by another 24 h of incubation. Subsequent steps, including cell fixation, permeabilization, and staining, were performed strictly following the manufacturer's protocols for the EdU assay kit. The experiment was independently repeated thrice. For each independent experiment, five randomly selected microscopic fields per group were analyzed, and the mean value of these fields was considered an independent experimental replicate.

Chromatin immunoprecipitation quantitative PCR (ChIP-qPCR)

ChIP-qPCR was performed using the ChIP-IT High Sensitivity kit (Active Motif, Cat. No. 53040) following the manufacturer's instructions. A549 cells were cultured to approximately 70%-80% confluence and cross-linked using a formaldehyde-containing fixation buffer. The cross-linking reaction was terminated using the supplied Stop Solution. Cells were collected, washed with ice-cold phosphate-buffered saline, and lysed in chromatin preparation buffer supplemented with protease inhibitors. The isolated chromatin was fragmented by sonication, and the size of the sheared DNA was confirmed to be approximately 200-1200 bp. Aliquots of fragmented chromatin were used as input controls. For immunoprecipitation, 10-30 μg of fragmented chromatin was incubated with 4 μg of anti-ETV5 antibody or normal rab-

bit IgG as a negative control at 4°C overnight. Protein G agarose beads were subsequently added, and the samples were incubated for an additional 3 h at 4°C with rotation. The immune complexes were collected and washed five times using the supplied washing buffer. The chromatin complexes were eluted, followed by reverse cross-linking and protein digestion with proteinase K. DNA was subsequently purified using DNA purification columns supplied with the kit. The purified DNA was subjected to quantitative PCR using primers flanking the predicted ETV5-binding region in the FOXA2 promoter. The FOXA2 promoter region was enriched in ETV5-immunoprecipitated chromatin relative to the IgG control.

Xenograft tumor model

Female nude mice aged 6-8 weeks and weighing approximately 18-22 g were randomly divided into vector control and ETV5-overexpression (ETV5-OE) groups (n = 6). A549 cells stably transduced with the control vector or ETV5-overexpression lentivirus were harvested during the logarithmic growth phase and resuspended in a Matrigel mixture. Approximately 5 × 10^6 cells in 100 μL were subcutaneously injected into the right flank of each mouse. After tumor establishment, tumor length and width were measured every 3 days with a digital caliper. Tumor volume was calculated using the formula V = (length × width^2)/2. Tumor growth was monitored on days 1, 4, 7, 10, 13, and 16. At the end of the experiment, the mice were anesthetized with isoflurane (3-5% for induction) to rapidly induce loss of consciousness, and were then euthanized by cervical dislocation. The xenograft tumors were subsequently removed, and the xenograft tumors were removed, photographed, and weighed. Tumor tissues were then processed for histological analysis. For immunohistochemistry, paraffin-embedded tumor sections were stained with antibodies against FOXA2, cleaved caspase-3, and Ki67. All animal experiments were approved by the Experimental Animal Welfare and Ethics Committee of the Affiliated Hospital of Zunyi Medical University (approval No. zyfyan-2026-0147) and were conducted according to institutional guidelines for animal care and use.

Data analysis

Statistical analyses were carried out using R software (version 4.2.1) and GraphPad Prism (version 10.4.2). Student's t-test was used to compare two independent groups at a single time point. For comparisons involving three or more groups at a single time point, one-way analysis of variance (ANOVA) was used, followed by Tukey's multiple-comparison test. For experiments with different treatment groups measured repeatedly over time, such as CCK-8 time-course assays and xenograft tumor growth curves, two-way repeated-measures ANOVA was used to assess the effects of treatment, time, and the treatment × time interaction. Survival analyses were performed using Kaplan-Meier curves with log-rank tests, whereas the independent prognostic value of ETV5 was further evaluated using multivariable Cox proportional hazards regression. Correlations between variables were assessed using Pearson or Spearman correlation analyses, as specified for each analysis. Continuous experimental data are presented as mean ± SD. All *in vitro* experiments were conducted in triplicate and independently repeated at least thrice. All tests were two-sided, and $P < 0.05$ was considered statistically significant. Statistical significance is indicated as $^{*}P < 0.05$, $^{**}P < 0.01$, $^{***}P < 0.001$, and $^{****}P < 0.0001$.

Results

Expression characteristics of ETV genes in LUAD

First, we analyzed the differential expression of ETV genes between LUAD and normal samples in the TCGA database. The results revealed that the expression levels of ETV1 and ETV5 were significantly higher in normal tissues compared to LUAD samples, whereas ETV4 expression was elevated in LUAD samples (**Figure 2A**). A heatmap depicting the correlation between ETV family gene expression and clinicopathological characteristics was generated to study associations with patient age (≤ 60 versus > 60 years), gender (F/M), and tumor stage (T1+T2 versus T3+T4; N0+N1 versus N2+N3; M0 versus M1; stage I+II versus III+IV). Although ETV1 and ETV4 revealed non-significant correlations with these clinical parameters, specific methylation sites of ETV5 exhibited a significant association with patient gender (**Figure 2B-D**). Kaplan-Meier survival analysis was performed to assess the relationship between the mRNA expression levels of ETV genes and OS. Higher expression of ETV1, ETV4, and ETV5 was asso-

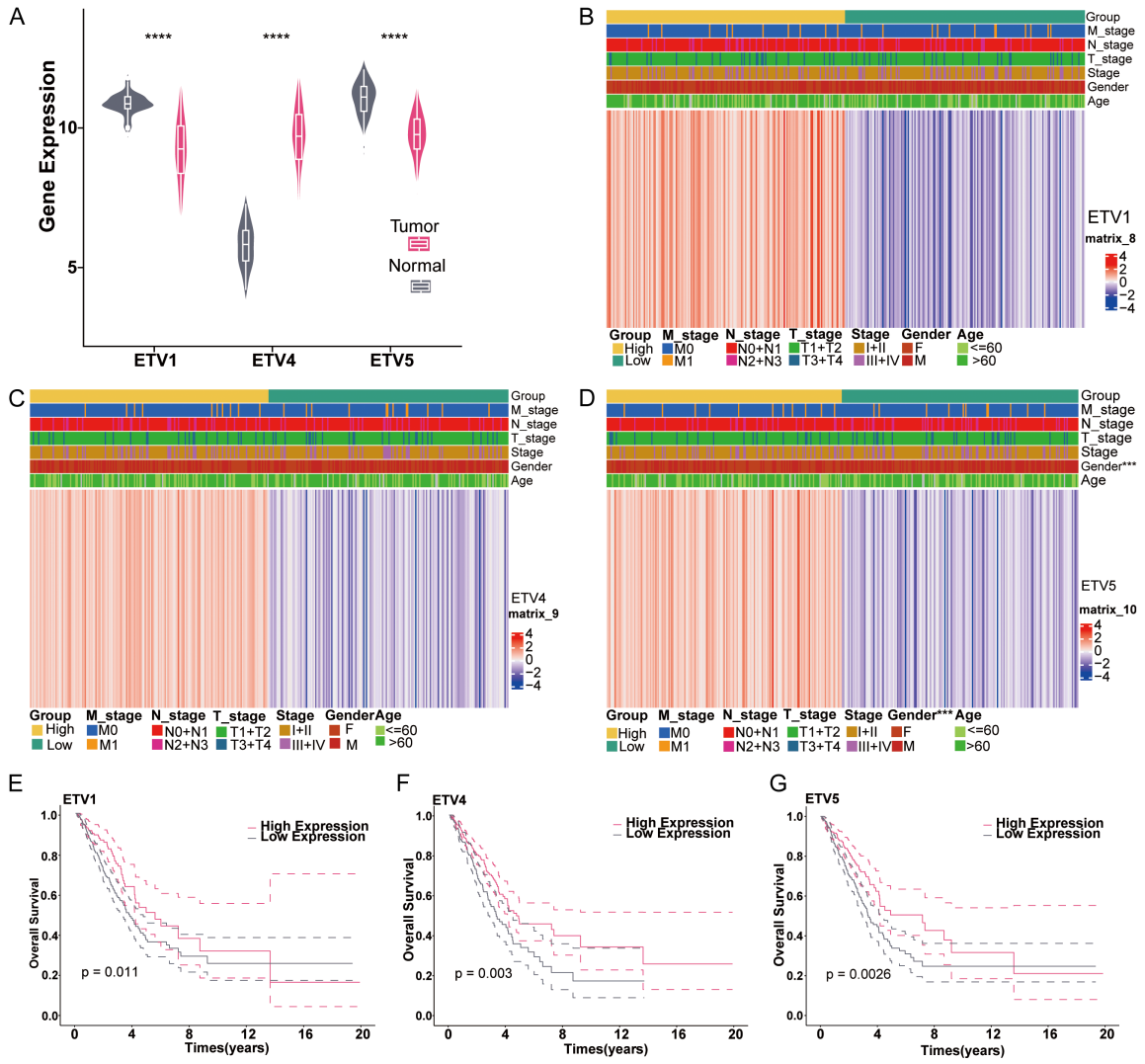

Figure 2. Expression characteristics of ETV genes in LUAD. (A) Differential expression of ETV1, ETV4, and ETV5 between LUAD tumors and adjacent normal tissues in the TCGA-LUAD cohort (541 tumors and 59 normal samples). (B-D) Heatmaps exhibiting the correlation between ETV1 (B), ETV4 (C), and ETV5 (D) expression levels and clinicopathological variables, including age, gender, tumor (T), node (N), metastasis (M) stages, and overall stage. (E-G) Kaplan-Meier overall survival curves stratified by high versus low mRNA expression of ETV1 (E), ETV4 (F), and ETV5 (G). Survival differences were tested by the log-rank test: ETV1, $P = 0.011$; ETV4, $P = 0.003$; ETV5, $P = 0.0026$. $^{*}P < 0.05$, $^{**}P < 0.01$, $^{***}P < 0.001$, $^{****}P < 0.0001$.

ciated with better survival in patients with LUAD (**Figure 2E-G**). This finding suggests that these genes may be linked to less aggressive disease progression.

Mutation characteristics of ETV genes

Given the reported involvement of ETV gene alterations in cancer, we examined the mutation profiles of ETV family members in LUAD and their associations with clinical features, including age, sex, stage, and prognosis. Among 533 LUAD samples, 9 (1.69%) carried mutations in ETV family genes. ETV5 mutations were detected in 1% of the samples, whereas no mutations were found in ETV1 or ETV4 (**Figure 3A**). Survival analysis showed no significant association between SNV status of ETV1 or ETV5 and overall survival (Figure S1A, S1B). We also examined copy number variation (CNV) patterns and their associations with clinical features and prognosis. ETV1 showed the highest amplification frequency and the lowest deletion frequency, whereas ETV5 showed the

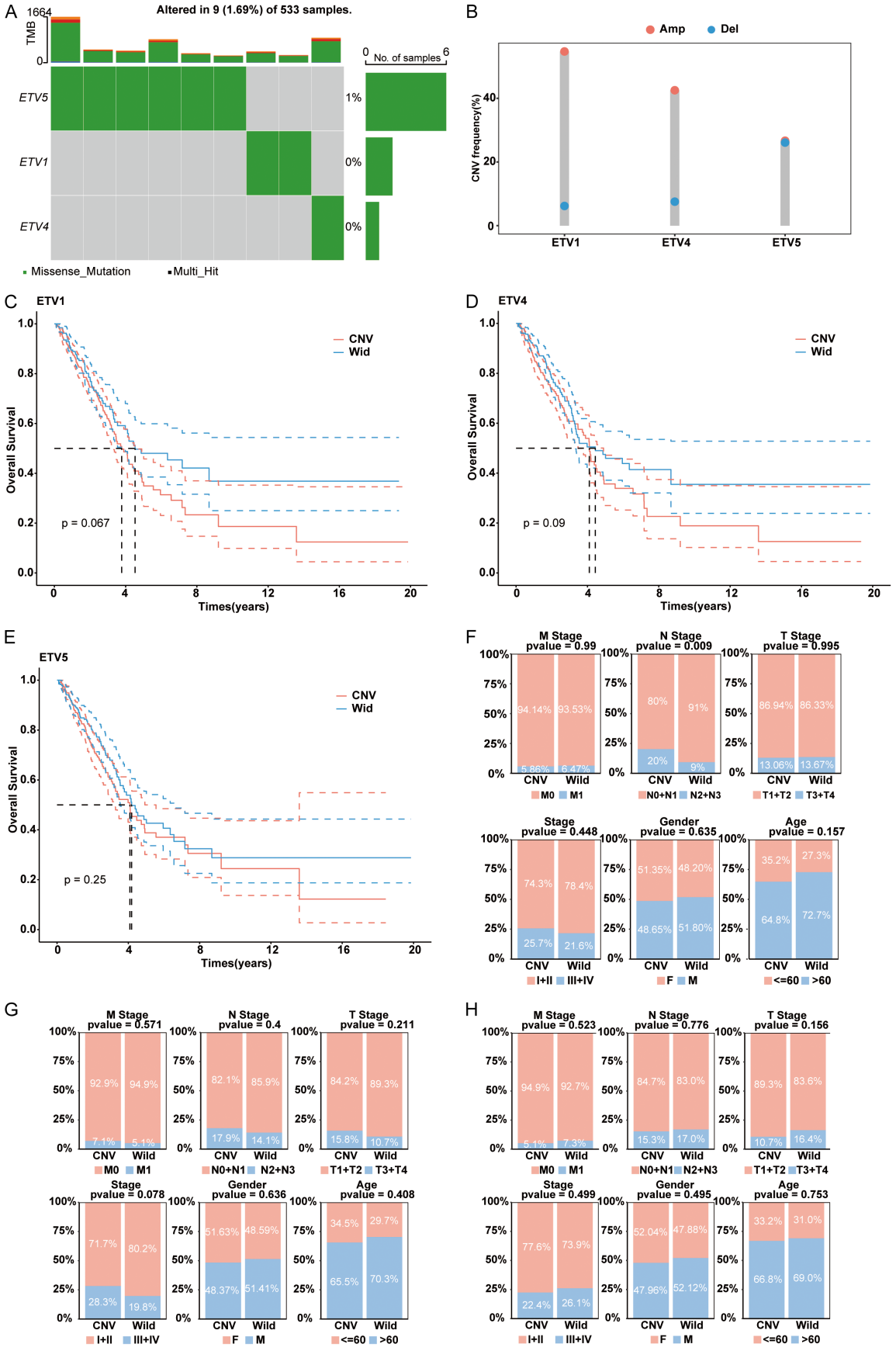
A
Altered in 9 (1.69%) of 533 samples.
TMB
1664
0
No. of samples
0
6
ETV5
ETV1
ETV4
1%
0%
0%
Missense_Mutation
Multi_Hit
B
Amp
Del
CNV frequency(%)
40
20
0
ETV1
ETV4
ETV5
C
ETV1
CNV
Wid
Overall Survival
p = 0.067
Times(years)
D
ETV4
CNV
Wid
Overall Survival
p = 0.09
Times(years)
E
ETV5
CNV
Wid
Overall Survival
p = 0.25
Times(years)
F
M Stage
pvalue = 0.99
94.14%
93.53%
5.86%
6.47%
M0
M1
N Stage
pvalue = 0.009
80%
91%
20%
9%
N0+N1
N2+N3
T Stage
pvalue = 0.995
86.94%
86.33%
13.06%
13.67%
T1+T2
T3+T4
Stage
pvalue = 0.448
74.3%
78.4%
25.7%
21.6%
I+II
III+IV
Gender
pvalue = 0.635
51.35%
48.20%
48.65%
51.80%
F
M
Age
pvalue = 0.157
35.2%
27.3%
64.8%
72.7%
<=60
>60
CNV
Wild
G
M Stage
pvalue = 0.571
92.9%
94.9%
7.1%
5.1%
N Stage
pvalue = 0.4
82.1%
85.9%
17.9%
14.1%
T Stage
pvalue = 0.211
84.2%
89.3%
15.8%
10.7%
Stage
pvalue = 0.078
71.7%
80.2%
28.3%
19.8%
Gender
pvalue = 0.636
51.63%
48.59%
48.37%
51.41%
Age
pvalue = 0.408
34.5%
29.7%
65.5%
70.3%
H
M Stage
pvalue = 0.523
94.9%
92.7%
5.1%
7.3%
N Stage
pvalue = 0.776
84.7%
83.0%
15.3%
17.0%
T Stage
pvalue = 0.156
89.3%
83.6%
10.7%
16.4%
Stage
pvalue = 0.499
77.6%
73.9%
22.4%
26.1%
Gender
pvalue = 0.495
52.04%
47.88%
47.96%
52.12%
Age
pvalue = 0.753
33.2%
31.0%
66.8%
69.0%

Figure 3. Mutation characteristics of ETV genes. (A) Single-nucleotide variant (SNV) mutation frequency of ETV family genes in TCGA-LUAD (533 samples). Nine samples (1.69%) harbored ETV family mutations: ETV5 1%, ETV1 0%, ETV4 0%. (B) CNV alteration frequency of ETV1, ETV4, and ETV5 in TCGA-LUAD. Amplification (Amp) means amplification, and deletion (Del) means deletion. (C-E) Kaplan-Meier survival analysis comparing CNV-altered versus wild-type (Wid) samples for ETV1 (C: $P = 0.067$), ETV4 (D: $P = 0.09$), and ETV5 (E: $P = 0.25$), assessed by the log-rank test. (F-H) Association between ETV1 (F), ETV4 (G), and ETV5 (H) CNV status and clinical parameters (M stage, N stage, T stage, overall stage, gender, and age).

opposite pattern. ETV4 had intermediate frequencies of both amplification and deletion (**Figure 3B**). These differences indicate that ETV family members have distinct CNV patterns in LUAD. Prognostic analysis revealed a non-significant association between CNV mutations in ETV family genes and OS (**Figure 3C-E**). Additionally, CNV mutations in ETV genes exhibited a non-significant impact on most clinical parameters, except for a significant correlation between ETV1 CNV and N stage. Higher ETV1 CNV mutation rates were associated with increased proportions of N2+N3 stages (**Figure 3F-H**), indicating that ETV1 CNV mutations may influence lymph node metastasis progression in patients.

Methylation characteristics of ETV genes

Given that ETV family genes frequently exhibit alterations in methylation sites in cancer [13, 17], we analyzed the relationship between methylation site variations in ETV genes and clinical parameters in LUAD. By examining the correlation between ETV family gene expression and clinicopathological features, we studied associations between methylation site alterations and patient age (≤ 60/> 60 years), gender (F/M), and tumor stage (T1+T2/T3+T4, N0+N1/N2+N3, M0/M1, and I+II/III+IV). Box plots were used to display the significant methylation sites and their methylation levels within the ETV family. For ETV1, eight methylation probes were identified, all exhibiting significant differences in methylation levels between tissue types. Among these, cg21463790 and cg26796083 exhibited higher methylation levels (β = 0.5-0.75) (**Figure 4A**). ETV4 exhibited only two probes, cg1200348 and cg24679082, with normal tissues demonstrating higher methylation levels than tumor tissues (**Figure 4B**). ETV5 presented three probes, with overall methylation levels significantly higher than those of ETV1 and ETV4 (**Figure 4C**). Analysis of the average gene methylation levels at significant sites revealed that ETV5 had higher average methylation than ETV1 and ETV4; however, only ETV4 revealed statistically significant differences in methylation levels between tissue types (**Figure 4D-F**). These results suggest that ETV5 may be more susceptible to aberrant methylation, potentially influencing gene expression and contributing to tumorigenesis, whereas the low ETV4 methylation level implies a weaker methylation-mediated regulation of its expression. Higher methylation levels of ETV family genes tended to be associated with shorter overall survival (OS). Among the three genes, only ETV1 methylation showed a significant association with patient survival ($P = 0.0077$). No significant relationship with OS was found for ETV4 or ETV5 methylation ($P > 0.05$) (**Figure 4G-I**). Methylation levels of the ETV family genes were also not significantly associated with the other clinical features examined (Figure S2A-C). Further correlation analysis revealed that the methylation levels of cg06518884 and cg07803284 were negatively associated with ETV5 mRNA expression (cg06518884: $r = -0.21$, $P < 0.001$; cg07803284: $r = -0.18$, $P < 0.001$), whereas cg04400533 was positively associated with ETV5 expression ($r = 0.21$, $P < 0.001$) (**Figure 4J-L**). Among these CpG sites, cg07803284 showed higher methylation in LUAD tissues and was negatively correlated with ETV5 expression. This pattern suggests that methylation at cg07803284 may partly contribute to the reduced expression of ETV5.

Single-cell analysis of ETV genes in LUAD

We analyzed the GSE131907 scRNA-seq dataset to examine the expression of ETV family genes across different cell populations. Feature plots were generated to show the expression patterns of ETV1, ETV4, and ETV5 (**Figure 5A**). Dot plot analysis revealed strong correlations between all three genes and the epithelial cell-related genes. Additionally, ETV1 was positively correlated with fibroblast-related genes, whereas ETV5 was positively correlated with dendritic cell-related genes (**Figure 5B**). Heatmap analysis demonstrated high ETV5 expression in

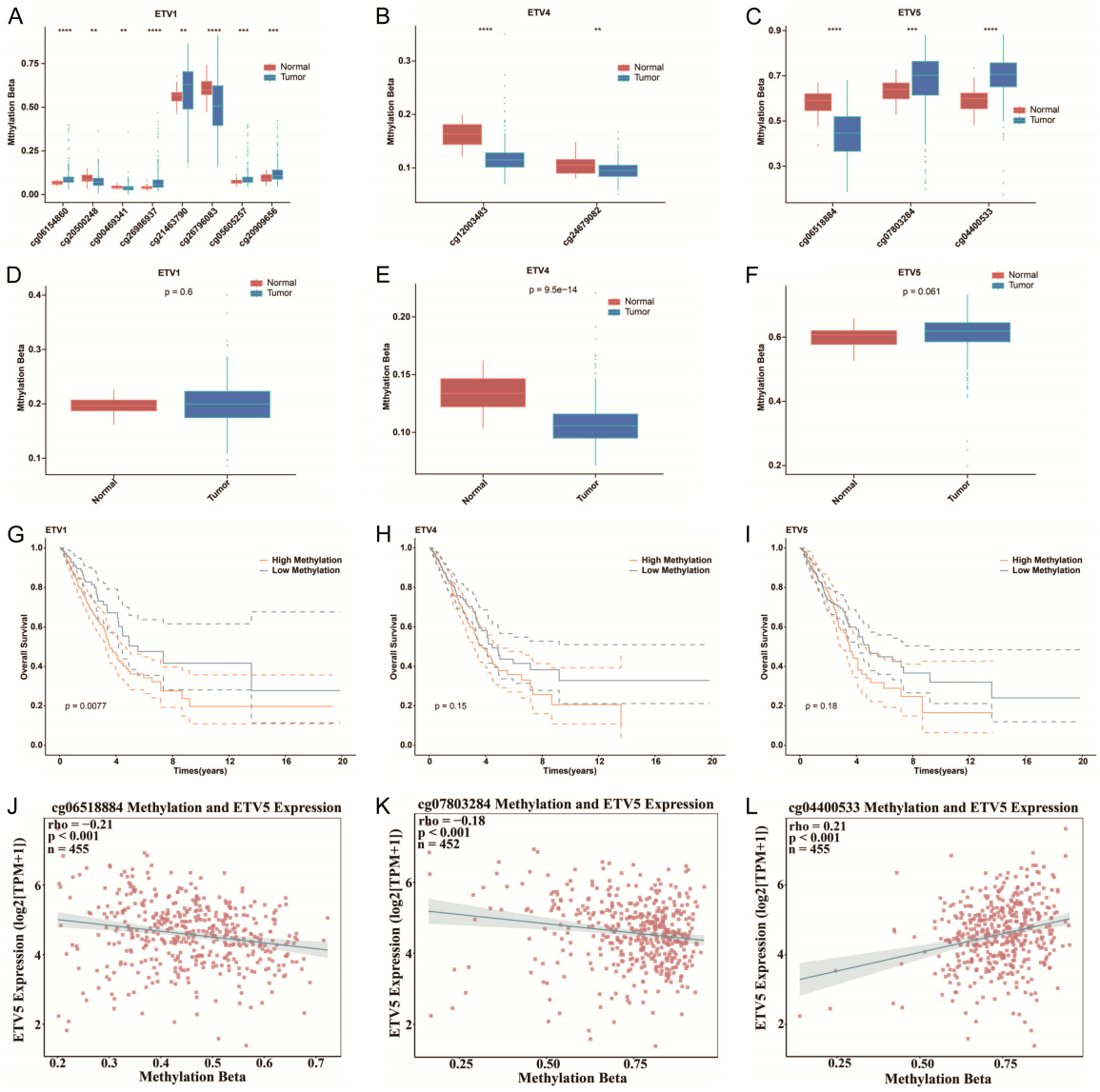

Figure 4. Methylation characteristics of ETV genes. (A-C) Methylation levels of significant CpG sites for ETV1 (A), ETV4 (B), and ETV5 (C) in tumor versus normal tissues from TCGA-LUAD. (D-F) Average methylation levels of significant sites for ETV1 (D: $P = 0.6$), ETV4 (E: $P = 9.5 \times 10^{-14}$), and ETV5 (F: $P = 0.061$), analyzed by the Wilcoxon rank-sum test. (G-I) Kaplan-Meier survival analysis based on mean methylation level of significant sites for ETV1 (G: $P = 0.0077$), ETV4 (H: $P = 0.15$), and ETV5 (I: $P = 0.18$). (J-L) Correlation analyses between ETV5 CpG methylation cg06518884 (J), cg07803284 (K), and cg04400533 (L) and ETV5 mRNA expression in TCGA-LUAD samples. The fitted line and shaded area represent the regression trend and 95% confidence interval, respectively. $^{*}P < 0.05$, $^{**}P < 0.01$, $^{***}P < 0.001$, $^{****}P < 0.0001$.

normal tissues, whereas ETV1 and ETV4 were predominantly expressed in tumor tissues (**Figure 5C**). Correlation analysis between gene expression and cell proportions indicated a generally high expression of ETV family genes in epithelial cells and fibroblasts; however, low expression in B cells and CD4 conventional T cells (**Figure 5D**). Furthermore, we conducted detailed analyses of the correlations between ETV1, ETV4, and ETV5 expressions and the proportions of different cell types (Figure S3). Finally, spatial expression heatmaps of ETV family genes in tissue sections revealed that ETV1 exhibited low and scattered expression throughout the tissues. ETV4 demonstrated a higher overall expression than ETV1, with more extensive high-expression regions. Among the three genes, ETV5 displayed the highest overall

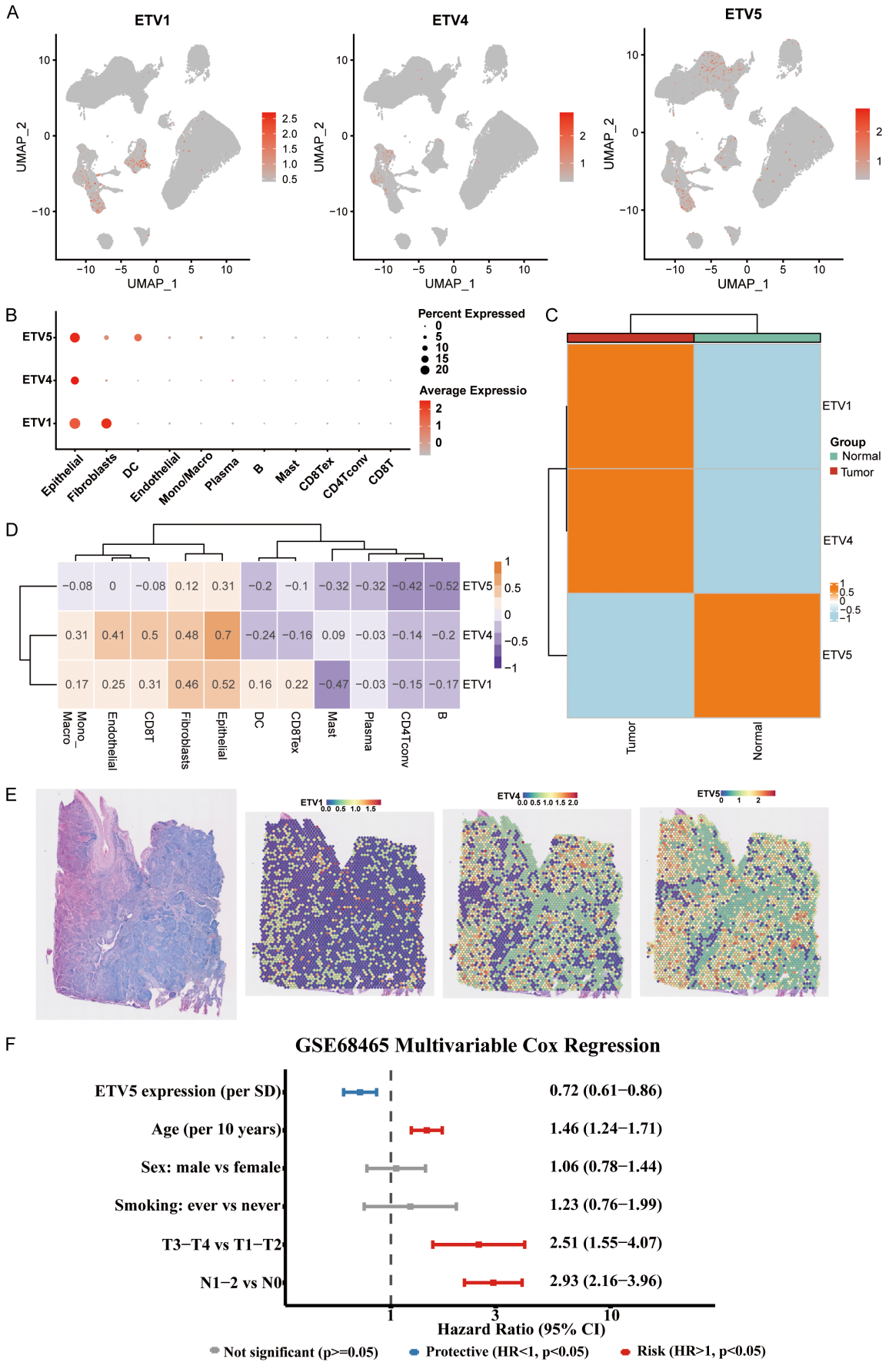
A
ETV1
ETV4
ETV5
UMAP_1
UMAP_2
B
Percent Expressed
Average Expressio
ETV5
ETV4
ETV1
Epithelial
Fibroblasts
DC
Endothelial
Mono/Macro
Plasma
B
Mast
CD8Tex
CD4Tconv
CD8T
C
Group
Normal
Tumor
ETV1
ETV4
ETV5
D
E
F
GSE68465 Multivariable Cox Regression
ETV5 expression (per SD)
Age (per 10 years)
Sex: male vs female
Smoking: ever vs never
T3−T4 vs T1−T2
N1−2 vs N0
0.72 (0.61−0.86)
1.46 (1.24−1.71)
1.06 (0.78−1.44)
1.23 (0.76−1.99)
2.51 (1.55−4.07)
2.93 (2.16−3.96)
Hazard Ratio (95% CI)
Not significant (p>=0.05)
Protective (HR<1, p<0.05)
Risk (HR>1, p<0.05)

Figure 5. Single-cell analysis of ETV genes in LUAD. A. Uniform Manifold Approximation and Projection feature plots depicting ETV1, ETV4, and ETV5 expression in single cells from the GEO dataset GSE131907 (11 tumor and 11 matched normal LUAD samples). B. Dot plot depicting ETV family gene expression across the annotated cell types. C. Heatmap of average ETV family gene expression in normal versus tumor tissues. D. Correlation heatmap between ETV family gene expression and cell-type proportions; Pearson correlation coefficients are presented. E. Spatial transcriptomic expression maps of ETV1, ETV4, and ETV5 in LUAD tissue sections from the SCAR database (dataset SCAR_ST_000010). F. Forest plot revealing HRs and 95% CIs for ETV5 expression and clinicopathological variables in the multivariable Cox proportional hazards model (HR = 0.72, 95% CI: 0.61-0.86).

expression level and the most concentrated high-expression regions in the tissues (**Figure 5E**). Next, we assessed whether ETV5 expression was independently associated with patient prognosis using multivariable Cox regression analysis in the GSE68465 cohort. After adjustment for clinical covariates, higher ETV5 expression remained significantly associated with a reduced risk of death (HR per SD increase = 0.72, 95% CI: 0.61-0.86), indicating that ETV5 expression is an independent favorable prognostic factor in LUAD. Conversely, increasing age (HR = 1.46, 95% CI: 1.24-1.71), advanced T stage (T3-T4 versus T1-T2: HR = 2.51, 95% CI: 1.55-4.07), and lymph node involvement (N1-N2 versus N0: HR = 2.93, 95% CI: 2.16-3.96) were independently associated with a poorer prognosis. Gender (HR = 1.06, 95% CI: 0.78-1.44) and smoking status (HR = 1.23, 95% CI: 0.76-1.99) were non-significantly associated with survival in the multivariable model (**Figure 5F**). These findings suggest that ETV5 may be more vital in the tissue microenvironment and could serve as a potential molecular marker at the tissue level.

Overexpression of ETV5 inhibited LUAD cell proliferation

Based on previous findings, we selected ETV5 as our primary target for further investigation. First, we detected ETV5 expression in human normal bronchial epithelial cells (BEAS-2B) and LUAD cells (A549). ETV5 expression was significantly higher in BEAS-2B cells than in A549 cells, which was consistent with our earlier observations (**Figure 6A**). We therefore generated an A549 cell line overexpressing ETV5 and confirmed the increase in ETV5 protein by Western blotting (**Figure 6B**). The CCK-8 assay showed that ETV5 overexpression reduced LUAD cell viability (**Figure 6C**), while the EdU assay showed a clear decrease in cell proliferation (**Figure 6D**). Flow cytometry also showed a higher apoptosis rate in ETV5-overexpressing cells than in vector control cells (**Figure 6E**). These results suggest that ETV5 overexpression suppresses cell growth and promotes apoptosis in A549 cells.

ETV5 upregulated FOXA2 expression

To explore how ETV5 affects LUAD cell proliferation, we screened potential transcriptional regulators and constructed a regulatory network (**Figure 7A**). Functional enrichment analysis was performed on the associated genes. GO enrichment analysis revealed that ETV5-related genes were positively associated with primitive hemopoiesis and platelet morphogenesis, while negatively correlated with functions including heterochromatin formation and DNA methylation (**Figure 7B**). KEGG pathway analysis indicated that ETV5-related genes were positively enriched in the Apelin signaling pathway and negatively associated with pathways, including Fanconi anemia (**Figure 7C**). FOXA2 is an important transcription factor that primarily functions as a tumor suppressor in LUAD [18]. The regulatory network (**Figure 7A**) suggested a positive regulatory relationship between FOXA2 and ETV5, leading us to hypothesize that ETV5 upregulates FOXA2 expression. We further examined their expression relationship in the GSE31210 LUAD cohort. Spearman correlation analysis revealed a significant positive correlation between ETV5 and FOXA2 expression across 226 LUAD samples (Spearman R = 0.53, $P < 0.001$) (**Figure 7D**). To test this hypothesis, we examined FOXA2 protein levels following ETV5 overexpression and observed that FOXA2 expression was significantly higher in the ETV5-OE group compared to the vector control group (**Figure 7E**). Furthermore, dual-luciferase reporter assays and ChIP-qPCR confirmed the positive regulation of FOXA2 by ETV5 (**Figure 7F**, **7G**).

ETV5 inhibited LUAD cell proliferation by upregulating FOXA2 expression

Building upon the confirmed positive regulation of FOXA2 by ETV5, we studied whether FOXA2 mediates the suppressive effects of ETV5 on

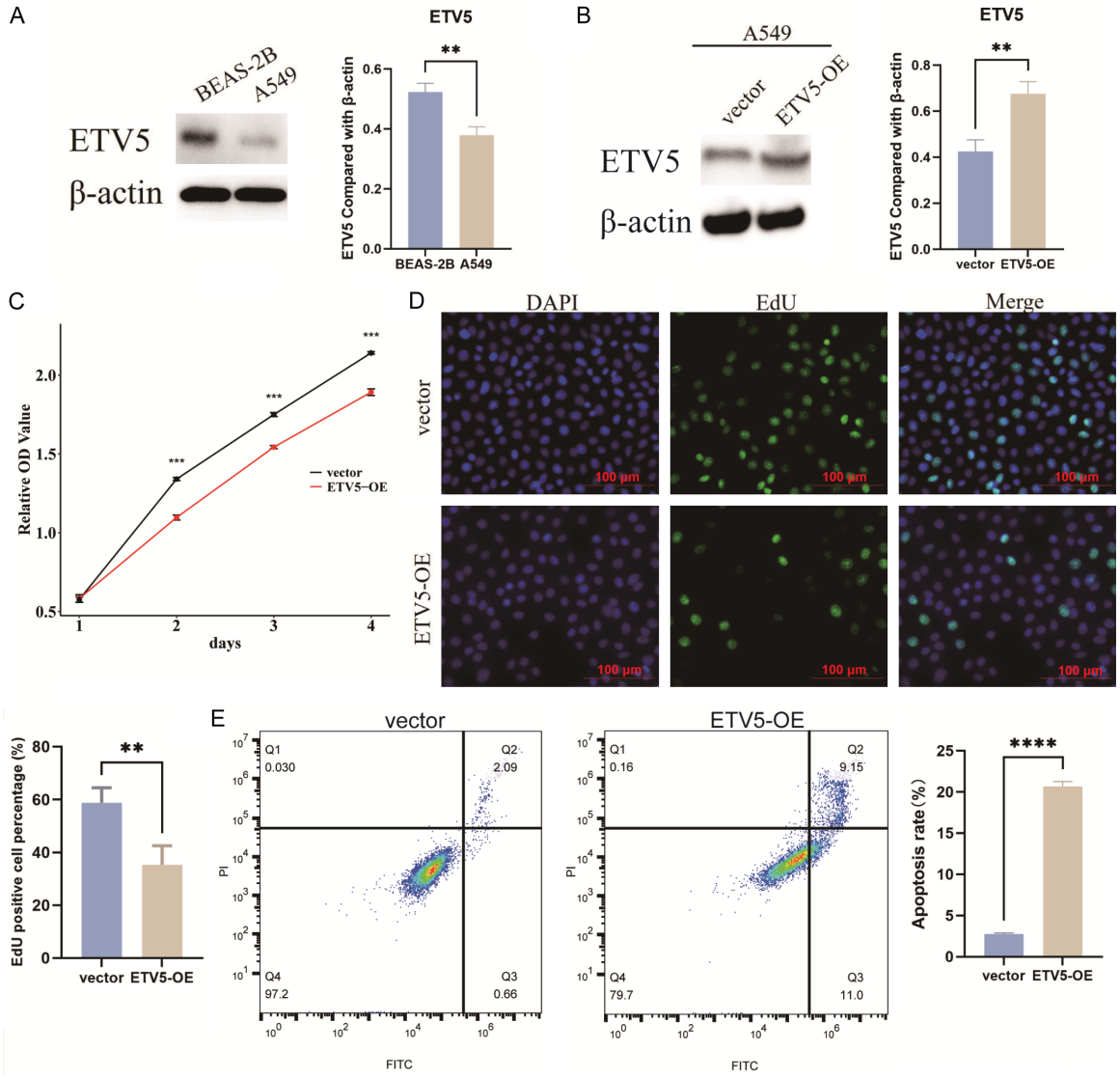

Figure 6. ETV5 overexpression inhibits LUAD cell proliferation. A. Western blotting assay was used to detect the protein expression of ETV5 in normal lung epithelial cells (BEAS-2B) and LUAD cells (A549). B. Western blotting was used to detect the overexpression efficiency of ETV5. C. CCK-8 was used to detect the effect of ETV5 overexpression on A549 cell viability. Statistical significance for the time-course data was assessed using two-way repeated-measures ANOVA. D. EdU assay was used to detect the effect of ETV5 overexpression on the proliferation of A549 cells. Magnification, 400×; 100 μm. E. Flow cytometry was used to detect the effect of ETV5 overexpression on apoptosis in A549 cells. Statistical significance was assessed using an unpaired two-tailed Student's t-test. $^{*}P < 0.05$, $^{**}P < 0.01$, $^{***}P < 0.001$.

LUAD cell proliferation. To test this hypothesis, we established a FOXA2 knockdown A549 cell line (siFOXA2) and confirmed knockdown efficiency by Western blotting (**Figure 8A**). Notably, FOXA2 knockdown with either siRNA did not significantly alter ETV5 protein expression (**Figure 8B**), supporting the notion that FOXA2 functions downstream of ETV5 rather than regulating ETV5 expression in a feedback manner. Subsequently, we concurrently knocked down FOXA2 in ETV5-overexpressing A549 cells. CCK-8 assays demonstrated that FOXA2 knockdown rescued the ETV5-induced reduction in cell viability (**Figure 8C**, **8E**). EdU incorporation assays further revealed that combined FOXA2 knockdown significantly restored the proliferative capacity impaired by ETV5 overexpression (**Figure 8D**, **8F**). Flow cytometry showed that FOXA2 knockdown reduced the increase in apoptosis caused by ETV5 overexpression (**Figure 8G**, **8H**). These results suggest that FOXA2 partly mediates the effects of ETV5 on

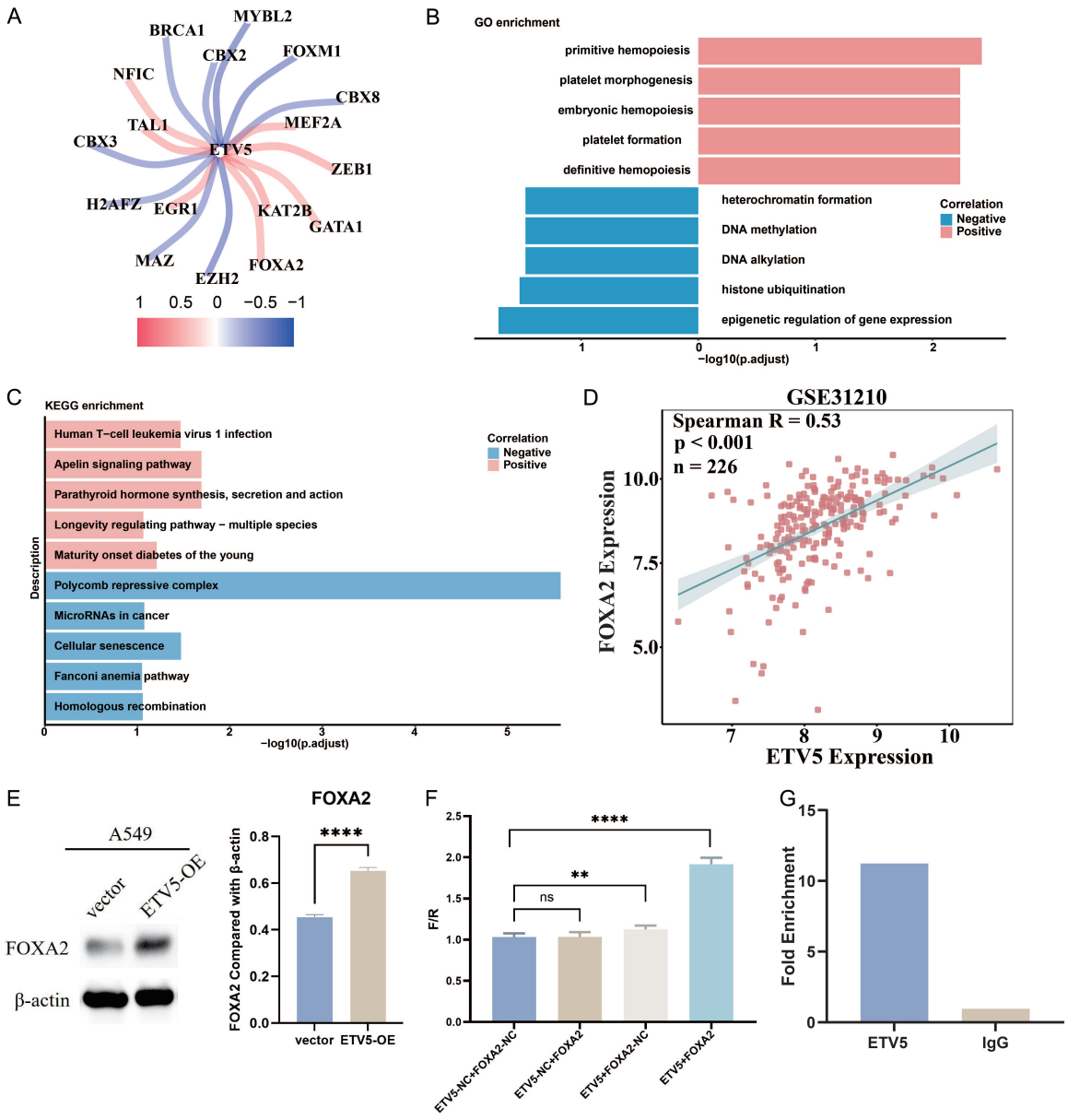

Figure 7. ETV5 upregulates FOXA2 expression. (A) ETV5 regulatory network constructed by integrating ENCODE transcription-factor targets and Pearson correlation analysis in the TCGA-LUAD cohort. (B, C) GO (B) and KEGG (C) enrichment analyses of ETV5-related genes. (D) Scatter plot exhibiting the association between ETV5 and FOXA2 expression in 226 LUAD samples from the GSE31210 dataset (R = 0.53, $P < 0.001$). The solid line represents the fitted regression trend, and the shaded area indicates the 95% CI. (E) Effect of ETV5 overexpression on FOXA2 protein expression by Western blotting assay. (F) Dual-luciferase assay verified the positive regulation of FOXA2 by ETV5. (G) ChIP-qPCR verified the positive regulation of FOXA2 by ETV5. $^{*}P < 0.05$, $^{**}P < 0.01$, $^{***}P < 0.001$.

LUAD cell proliferation and survival, and this relationship was observed in both LUAD cell lines.

ETV5 overexpression suppressed LUAD tumor growth in vivo

To examine whether the effects of ETV5 observed in vitro were also present in vivo, we established a subcutaneous xenograft model using A549 cells stably overexpressing ETV5 or the corresponding vector control. Tumors formed by ETV5-overexpressing cells were visibly smaller than those in the control group (Figure S4A). Tumor growth monitoring showed that ETV5 overexpression significantly reduced tumor volume, and this difference became apparent from day 7 (Figure S4B). At the end of

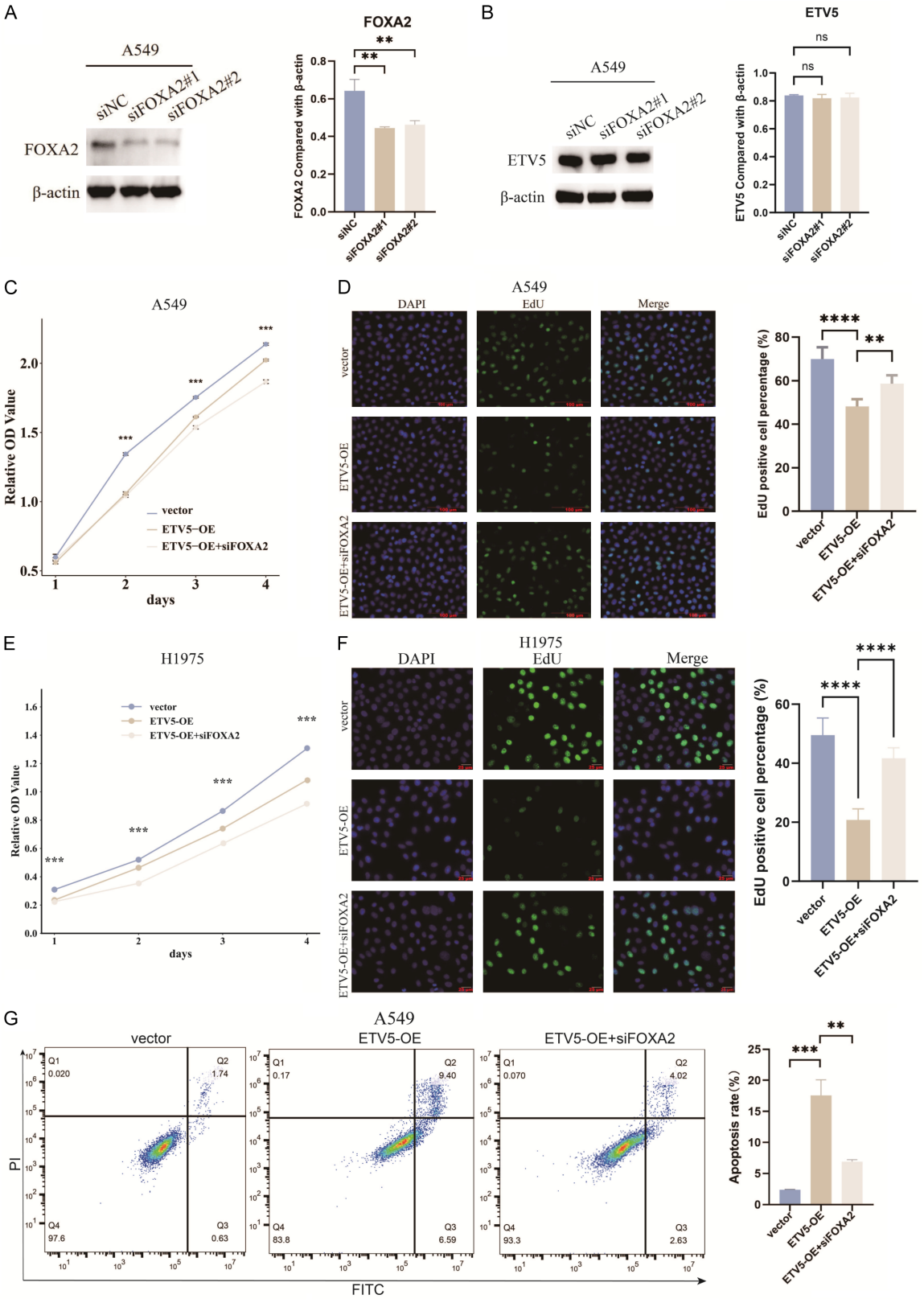
A
A549
siNC
siFOXA2#1
siFOXA2#2
FOXA2
β-actin
FOXA2
FOXA2 Compared with β-actin
B
A549
siNC
siFOXA2#1
siFOXA2#2
ETV5
β-actin
ETV5
ETV5 Compared with β-actin
ns
C
A549
Relative OD Value
days
vector
ETV5−OE
ETV5−OE+siFOXA2
D
A549
DAPI
EdU
Merge
vector
ETV5-OE
ETV5-OE+siFOXA2
EdU positive cell percentage (%)
E
H1975
Relative OD Value
days
vector
ETV5-OE
ETV5-OE+siFOXA2
F
H1975
DAPI
EdU
Merge
vector
ETV5-OE
ETV5-OE+siFOXA2
EdU positive cell percentage (%)
G
A549
vector
ETV5-OE
ETV5-OE+siFOXA2
PI
FITC
Q1 0.020
Q2 1.74
Q4 97.6
Q3 0.63
Q1 0.17
Q2 9.40
Q4 83.8
Q3 6.59
Q1 0.070
Q2 4.02
Q4 93.3
Q3 2.63
Apoptosis rate (%)

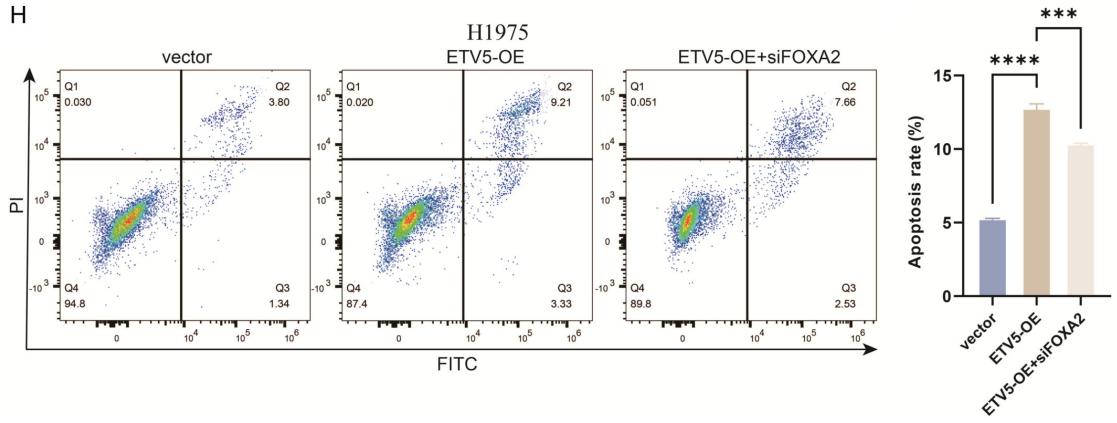

Figure 8. ETV5 inhibits LUAD cell proliferation by upregulating FOXA2 expression. A. Western blotting was used to verify the knockdown efficiency of FOXA2. B. Western blotting analysis of ETV5 expression following FOXA2 knockdown in A549 cells. C. CCK-8 was used to detect the effects of simultaneous overexpression of ETV5 and FOXA2 knockdown on viability in A549 cells. D. EdU was used to detect the effects of simultaneous ETV5 overexpression and FOXA2 knockdown on proliferation in A549 cells. Magnification, 400×; Scale bars, 100 μm. E. CCK-8 was used to detect the effects of simultaneous overexpression of ETV5 and knockdown of FOXA2 on viability in H1975 cells. For CCK-8 time-course analyses, statistical significance was evaluated using a two-way repeated-measures ANOVA. F. EdU was used to detect the effects of simultaneous ETV5 overexpression and FOXA2 knockdown on the proliferation of H1975 cells. Magnification, 400×; Scale bars, 25 μm. G. Flow cytometry was used to detect the effects of simultaneous overexpression of ETV5 and knockdown of FOXA2 on apoptosis in A549 cells. H. Flow cytometry was used to detect the effects of simultaneous ETV5 overexpression and FOXA2 knockdown on apoptosis in H1975 cells. $^{*}P < 0.05$, $^{**}P < 0.01$, $^{***}P < 0.001$.

the experiment, both tumor weight and tumor volume were significantly lower in the ETV5-OE group than in the vector control group (Figure S4C, S4D). These results indicate that ETV5 overexpression suppresses LUAD tumor growth *in vivo*. Immunohistochemical analysis revealed markedly increased FOXA2 expression in ETV5-overexpressing xenografts, consistent with the positive regulation of FOXA2 by ETV5 observed *in vitro*. Moreover, ETV5-overexpressing tumors exhibited increased cleaved caspase-3 staining and markedly decreased Ki67 staining compared with control tumors (Figure S4E). These results indicate that ETV5 overexpression inhibits tumor cell proliferation and is associated with enhanced apoptotic activity *in vivo*. Collectively, the xenograft data further support the tumor-suppressive role of ETV5 in LUAD and are consistent with the activation of ETV5-FOXA2 regulatory axis.

Discussion

By analyzing the TCGA database, we examined the differential expression of ETV family genes between LUAD and normal samples. Analysis revealed that ETV1 and ETV5 expression levels were significantly elevated in normal tissues compared to tumor tissues; however, ETV4 expression was higher in tumor tissues. Furthermore, survival analysis suggested that higher ETV1 and ETV5 expressions were associated with longer overall patient survival. *In vitro* experiments further validated the tumor-suppressive role of ETV5 in LUAD. The functions of ETV family members in cancer are context-specific. Multiple studies have demonstrated the tumor-promoting role of ETV4 in various cancers. For instance, ETV4 promotes thyroid cancer cell proliferation by upregulating tripartite motif containing 63 expression and subsequently activating threonine kinase 1 (AKT) signaling pathways [19]. Furthermore, ETV4's positive regulation of solute carrier family 7 member 11 facilitates the progression of papillary thyroid carcinoma, involving alterations in ferroptosis [20]. In colorectal cancer, ETV4 binding to the solute carrier family 38 member 5 (SLC38A5) promoter region enhances its transcription, thereby promoting cancer cell proliferation, glycolysis, and overall colorectal cancer progression [21]. Research on ETV1 in cancer is relatively limited; one study reported positive ETV1 expression in a tumor of a patient with gastric cancer, suggesting its potential as a diagnostic marker [22]. In colorectal cancer,

ETV5 has been reported to promote tumor cell proliferation and regulate cell-cycle progression [23]. ETV5 has also been reported to promote neuroendocrine differentiation and a more aggressive phenotype in prostate cancer [24]. In contrast, our findings suggest that ETV5 has a tumor-suppressive role in LUAD, indicating that the functions of ETV family members may vary across different tissue types.

Analysis of the mutational landscape of ETV1, ETV4, and ETV5 revealed that CNV is a relatively frequent alteration. Notably, the CNV status of ETV1 was significantly correlated with tumor N stage, suggesting its potential clinical relevance. Aberrations in ETV family genes have been reported in various tumors. For example, truncating mutations in ETV1 are observed in approximately 10% of prostate cancers and may promote disease progression [25]. ETV6 exon fusions are associated with the pathogenesis of myeloid neoplasms [26], and specific ETV family translocations aid in characterizing the differentiation lineage in Ewing sarcoma [27]. These findings collectively illustrate the diverse mutational patterns and potential biological effects of ETV genes across different tumor types.

Methylation is vital to LUAD pathogenesis. For instance, insulin-like growth factor 2 mRNA-binding protein 2-mediated m6A methylation of FLT4 enhances its mRNA stability, activating downstream signaling pathways and promoting LUAD migration and angiogenesis [28]. SET domain containing 1A-mediated methylation of Yes1-associated transcriptional regulator impedes its nuclear translocation, thereby promoting fibrinogen-like 1 transcription and enabling LUAD cells to evade immune cytotoxicity [29]. Given the importance of methylation in LUAD, researchers have identified methylation-driven mRNAs and long non-coding RNAs from hundreds of LUAD and adjacent normal tissues, constructing a prognostic model based on these RNAs, which provides potential biomarkers for early diagnosis [30]. Current research on the methylation of ETV family members is limited. We characterized the basic features of ETV methylation sites in LUAD and identified differentially methylated sites between LUAD and normal samples. We observed that the three methylation sites in ETV5 generally exhibited higher methylation levels than those in ETV1 and ETV4, providing a theoretical foundation and direction for future studies into the methylation mechanism of ETV5.

To explore the mechanism by which ETV5 influences LUAD, we screened for transcription factors potentially involved in its transcriptional regulation. *In vitro* experiments demonstrated that ETV5 positively regulates FOXA2 expression and that FOXA2 is involved in ETV5-mediated suppression of LUAD cell proliferation. FOXA2, a transcription factor belonging to the “pioneer factor” family, can initially bind to tightly packed chromatin, opening DNA access for other transcription factors and thereby initiating or modulating gene expression programs [31]. The role of FOXA2 in LUAD appears to depend on the biological context, although many studies support a tumor-suppressive function. Low FOXA2 expression has been associated with poor patient survival. In addition, loss of FOXA2 together with NK2 homeobox 1 and caudal type homeobox 2 has been reported to promote metastatic behavior in LUAD cells [32]. HOX transcript antisense RNA has been reported to regulate the FOXA1/FOXA2 ratio, which is associated with LUAD cell migration and invasion. Changes in this ratio may therefore affect LUAD progression [33]. FOXA2 loss has also been linked to epithelial-mesenchymal transition and increased LUAD metastasis through glycosylation-related post-translational modifications [34]. These findings are consistent with our results and further support a tumor-suppressive role for FOXA2 in LUAD. Additionally, our series of *in vitro* experiments confirmed that ETV5 inhibits LUAD cell viability and proliferation by upregulating FOXA2; targeting the ETV5/FOXA2 signaling pathway may therefore hold therapeutic potential in LUAD.

This study elucidates the tumor-suppressive role of ETV5 in LUAD by investigating the expression patterns, mutational profiles, methylation status, and biological functions of ETV family genes. However, this study has several limitations. First, the research primarily relies on retrospective analysis of public databases, which may introduce sample selection bias. The overall mutation frequency of ETV family genes is low, potentially limiting the statistical power to detect significant associations with clinical parameters. We acknowledge that the single-cell and spatial transcriptomic analyses presented here are correlative and do not pro-

vide direct evidence for the cell-type-specific activity of the ETV5-FOXA2 axis. Particularly, they do not allow unequivocal discrimination between malignant and normal epithelial cells, nor do they fully exclude potential contributions from stromal or immune cells. Direct validation by multiplex immunofluorescence, immunohistochemistry, or RNAscope co-staining for ETV5, FOXA2, and epithelial/tumor markers in LUAD tissue sections will be essential in future studies. Second, although this study confirms that ETV5 inhibits tumor proliferation by upregulating FOXA2, the upstream regulatory mechanisms and specific downstream signaling pathways remain incompletely characterized. Although enrichment analysis hinted at potential pathways such as Apelin signaling, the precise functional connection between these pathways and the ETV5-FOXA2 axis was not experimentally verified, leaving the regulatory network relatively preliminary. Third, the lack of *in vivo* experiments means that the tumor-suppressive effect of the ETV5/FOXA2 axis in the tumor microenvironment and at the organismal level remains unconfirmed. This study was mainly based on the A549 cell line, so the role of ETV5 in LUAD cells with different genetic backgrounds remains unclear. This limitation may reduce the generalizability of our findings. Future studies should include additional LUAD models, in vivo validation, and further mechanistic experiments to confirm and extend these results and to assess their potential clinical relevance.

Conclusion

By combining multi-omics analysis with experimental validation, this study characterized the expression patterns and biological roles of ETV family genes in LUAD. ETV1 and ETV5 showed higher expression in normal tissues, whereas ETV4 was more highly expressed in tumor tissues. Higher expression of all three genes was associated with better patient survival. ETV1 copy number amplification was significantly associated with lymph node metastasis, while higher ETV1 methylation was linked to shorter survival. Single-cell and spatial transcriptomic analyses showed distinct expression patterns of ETV5 within the tumor microenvironment. Functional experiments further showed that ETV5 overexpression reduced LUAD cell proliferation and increased apoptosis. ETV5 also promoted FOXA2 expression through direct transcriptional regulation. FOXA2 knockdown partly reversed the effects of ETV5 on cell proliferation and apoptosis. These findings suggest that the ETV5-FOXA2 axis is involved in the regulation of LUAD progression and may help improve our understanding of ETV-related transcriptional regulation in this disease.

Acknowledgements

During the language editing and proofreading stage of this manuscript, the authors used ChatGPT (OpenAI, GPT-4 model) to check grammar, spelling, and fluency. This AI tool was used solely for language improvement and did not participate in study design, data collection, data analysis, or conclusion generation. All AI-assisted edits have been reviewed and verified by the authors, who assume full responsibility for the entire manuscript content. No breach of publication ethics or academic misconduct is involved.

Disclosure of conflict of interest

None.

Address correspondence to: Hao Li, Department of Oncology I Public Health Treatment Centre No. 160 North Section, Huaxi Avenue Nanming District, Guiyang 550033, Guizhou, China. E-mail: 18984148083@163.com

References

[1] Smolarz B, Łukasiewicz H, Samulak D, Piekarska E, Kołacinski R and Romanowicz H. Lung cancer-epidemiology, pathogenesis, treatment and molecular aspect (review of literature). Int J Mol Sci 2025; 26: 2049.

[2] Bray F, Laversanne M, Sung H, Ferlay J, Siegel RL, Soerjomataram I and Jemal A. Global cancer statistics 2022: GLOBOCAN estimates of incidence and mortality worldwide for 36 cancers in 185 countries. CA Cancer J Clin 2024; 74: 229-263.

[3] Warth A, Muley T, Meister M, Stenzinger A, Thomas M, Schirmacher P, Schnabel PA, Budczies J, Hoffmann H and Weichert W. The novel histologic International Association for the Study of Lung Cancer/American Thoracic Society/European Respiratory Society classification system of lung adenocarcinoma is a stage-independent predictor of survival. J Clin Oncol 2012; 30: 1438-1446.

[4] Takeno N, Tarumi S, Abe M, Suzuki Y, Kinoshita I and Kato T. Lung adenocarcinoma with micro-

papillary and solid patterns: Recurrence rate and trends. Thorac Cancer 2023; 14: 2987-2992.
[5] Du Y, Cui X, Sidorenkov G, Groen HJM, Vliegenthart R, Heuvelmans MA, Liu S, Oudkerk M and de Bock GH. Lung cancer occurrence attributable to passive smoking among never smokers in China: a systematic review and meta-analysis. Transl Lung Cancer Res 2020; 9: 204-217.
[6] Florez N, Kiel L, Riano I, Patel S, DeCarli K, Dhawan N, Franco I, Odai-Afotey A, Meza K, Swami N, Patel J and Sequist LV. Lung cancer in women: the past, present, and future. Clin Lung Cancer 2024; 25: 1-8.
[7] Hubaux R, Becker-Santos DD, Enfield KS, Lam S, Lam WL and Martinez VD. Arsenic, asbestos and radon: emerging players in lung tumorigenesis. Environ Health 2012; 11: 89.
[8] Brey C, Gouveia FT, Silva BS, Sarquis LMM, Miranda FMD and Consonni D. Lung cancer related to occupational exposure: an integrative review. Rev Gaucha Enferm 2020; 41: e20190378.
[9] Ma Y, Du Y, Wang R, Ji X, Wu J, Liu Y, Guo X and Zhang Y. Analysis of multigene detection in patients with advanced lung adenocarcinoma using cytological specimens. Pathol Res Pract 2020; 216: 153036.
[10] Shang J, Jiang H, Zhao Y, Yang J, Lin Y, Zhang N, Ren L, Chen Q, Yu Y, Shi L, Li Y, Chen H and Zheng Y. Molecular subtyping of stage I lung adenocarcinoma via molecular alterations in pre-invasive lesion progression. J Transl Med 2025; 23: 263.
[11] Currie SL, Lau DKW, Doane JJ, Whitby FG, Okon M, McIntosh LP and Graves BJ. Structured and disordered regions cooperatively mediate DNA-binding autoinhibition of ETS factors ETV1, ETV4 and ETV5. Nucleic Acids Res 2017; 45: 2223-2241.
[12] Oh S, Shin S and Janknecht R. ETV1, 4 and 5: an oncogenic subfamily of ETS transcription factors. Biochim Biophys Acta 2012; 1826: 1-12.
[13] Sizemore GM, Pitarresi JR, Balakrishnan S and Ostrowski MC. The ETS family of oncogenic transcription factors in solid tumours. Nat Rev Cancer 2017; 17: 337-351.
[14] Adler D, Ochsenfahrt J, Fuchs K, Kristiansen G, Perner S and Wernert N. ERG is specifically associated with ETS-2 and ETV-4, but not with ETS-1, in prostate cancer. Int J Mol Med 2012; 30: 1029-1033.
[15] Raskin GA, Pozharisski KM, Iyevleva AG, Rikov IV, Orlova RV and Imyanitov EN. Unusual clinical presentation of gastrointestinal clear cell sarcoma. Gastrointest Tumors 2015; 2: 83-88.
[16] Birner P, Berghoff AS, Dinhof C, Pirker C, Capper D, Schoppmann SF, Petzelbauer P, von Deimling A, Berger W and Preusser M. MAP kinase activity supported by BRAF (V600E) mutation rather than gene amplification is associated with ETV1 expression in melanoma brain metastases. Arch Dermatol Res 2014; 306: 873-884.
[17] Oh S, Song H, Freeman WM, Shin S and Janknecht R. Cooperation between ETS transcription factor ETV1 and histone demethylase JMJD1A in colorectal cancer. Int J Oncol 2020; 57: 1319-1332.
[18] Tang Y, Shu G, Yuan X, Jing N and Song J. FOXA2 functions as a suppressor of tumor metastasis by inhibition of epithelial-to-mesenchymal transition in human lung cancers. Cell Res 2011; 21: 316-326.
[19] He J, Zhang Y, Yao B, Wang L and Tian Z. Tripartite motif containing 63, regulated by E26 transformation specific variant 4, facilitates the thyroid carcinoma progression and the AKT, p38, and ERK signaling pathways. Mol Cell Endocrinol 2022; 550: 111639.
[20] Wang L, Zhang Y, Yang J, Liu L, Yao B, Tian Z and He J. The knockdown of ETV4 inhibits the papillary thyroid cancer development by promoting ferroptosis upon SLC7A11 downregulation. DNA Cell Biol 2021; 40: 1211-1221.
[21] Huang Y, He J, Chen N, Du X and Peng J. ETV4 promotes the growth, metastasis, glycolysis, and oxaliplatin resistance of colorectal cancer by transcription activation-mediated SLC38A5 upregulation. Pathol Res Pract 2025; 271: 156033.
[22] Jung M, Park SH, Jeon YK, Won JK, Yang HK and Kim WH. Gastrointestinal stromal tumor of unusual phenotype after imatinib treatment: a case report and diagnostic utility of ETV1 mRNA in situ hybridization. Medicine (Baltimore) 2017; 96: e9031.
[23] Peng Y, Feng H, Wang C, Song Z, Zhang Y, Liu K, Cheng X and Zhao R. The role of E26 transformation-specific variant transcription factor 5 in colorectal cancer cell proliferation and cell cycle progression. Cell Death Dis 2021; 12: 427.
[24] Lee J, Park J, Hur Y, Um D, Choi HS, Park J, Kim Y, Lee JS, Choi K, Kim E, Park YB, Choi JM, Kim TK and Lee Y. ETV5 reduces androgen receptor expression and induces neural stem-like properties during neuroendocrine prostate cancer development. Proc Natl Acad Sci U S A 2025; 122: e2420313122.
[25] Morsalin S, Yang C, Fang J, Reddy S, Kayarthodi S, Childs E, Matthews R, Rao VN and Reddy ESP. Molecular mechanism of β-catenin signaling pathway inactivation in ETV1-positive prostate cancers. J Pharm Sci Pharmacol 2015; 2: 208-216.

[26] Beverloo HB, Panagopoulos I, Isaksson M, van Wering E, van Drunen E, de Klein A, Johansson B and Slater R. Fusion of the homeobox gene HLXB9 and the ETV6 gene in infant acute myeloid leukemias with the t(7;12)(q36;p13). Cancer Res 2001; 61: 5374-5377.
[27] Szuhai K, IJszenga M, Tanke HJ, Taminiau AH, de Schepper A, van Duinen SG, Rosenberg C and Hogendoorn PC. Detection and molecular cytogenetic characterization of a novel ring chromosome in a histological variant of Ewing sarcoma. Cancer Genet Cytogenet 2007; 172: 12-22.
[28] Fang H, Sun Q, Zhou J, Zhang H, Song Q, Zhang H, Yu G, Guo Y, Huang C, Mou Y, Jia C, Song Y, Liu A, Song K, Lu C, Tian R, Wei S, Yang D, Chen Y, Li T, Wang K, Yu Y, Lv Y, Mo K, Sun P, Yu X and Song X. m(6)A methylation reader IGF2BP2 activates endothelial cells to promote angiogenesis and metastasis of lung adenocarcinoma. Mol Cancer 2023; 22: 99.
[29] Jiang J, Ye P, Sun N, Zhu W, Yang M, Yu M, Yu J, Zhang H, Gao Z, Zhang N, Guo S, Ji Y, Li S, Zhang C, Miao S, Chai M, Liu W, An Y, Hong J, Wei W, Zhang S and Qiu H. Yap methylation-induced FGL1 expression suppresses anti-tumor immunity and promotes tumor progression in KRAS-driven lung adenocarcinoma. Cancer Commun (Lond) 2024; 44: 1350-1373.
[30] Li R, Yang YE, Yin YH, Zhang MY, Li H and Qu YQ. Methylation and transcriptome analysis reveal lung adenocarcinoma-specific diagnostic biomarkers. J Transl Med 2019; 17: 324.
[31] Liu N, Wang A, Xue M, Zhu X, Liu Y and Chen M. FOXA1 and FOXA2: the regulatory mechanisms and therapeutic implications in cancer. Cell Death Discov 2024; 10: 172.
[32] Li CM, Gocheva V, Oudin MJ, Bhutkar A, Wang SY, Date SR, Ng SR, Whittaker CA, Bronson RT, Snyder EL, Gertler FB and Jacks T. Foxa2 and Cdx2 cooperate with Nkx2-1 to inhibit lung adenocarcinoma metastasis. Genes Dev 2015; 29: 1850-1862.
[33] Wang R, Shi Y, Chen L, Jiang Y, Mao C, Yan B, Liu S, Shan B, Tao Y and Wang X. The ratio of FoxA1 to FoxA2 in lung adenocarcinoma is regulated by LncRNA HOTAIR and chromatin remodeling factor LSH. Sci Rep 2015; 5: 17826.
[34] Ge W, Wen S, Zhou X, Chen Y, Zeng D, Jiang J and Yang S. FOXA2 loss in TGF-β1-induced EMT suppresses bisecting-GlcNAc N-Glycan synthesis in lung adenocarcinoma. Proteomics 2025; 25: e202400216.

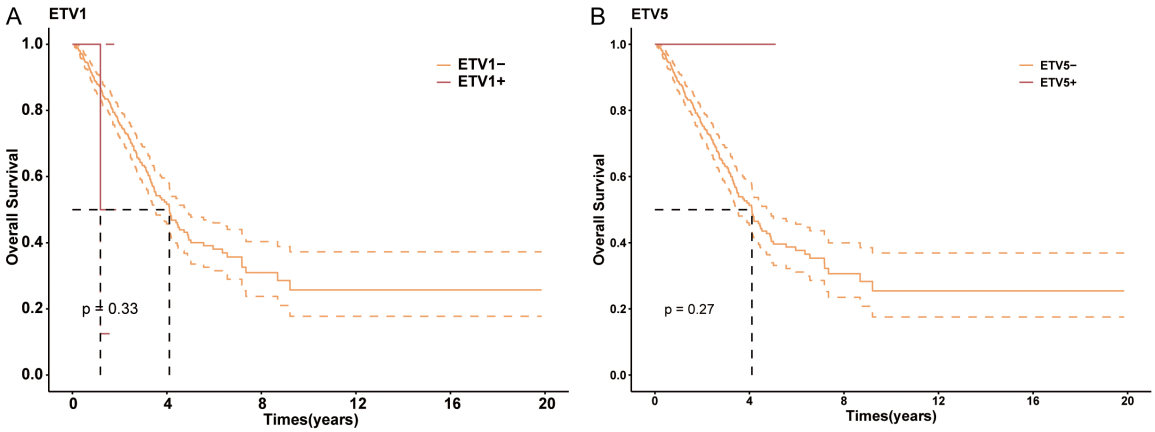

Figure S1. Association of ETV1 and ETV5 expression with survival outcomes. A, B. Kaplan-Meier OS curves comparing SNV-mutant (ETV1+/ETV5+) versus wild-type (ETV1-/ETV5-) samples in TCGA-LUAD (533 samples). Differences were tested by the log-rank test: ETV1, *P* = 0.33; ETV5, *P* = 0.27.

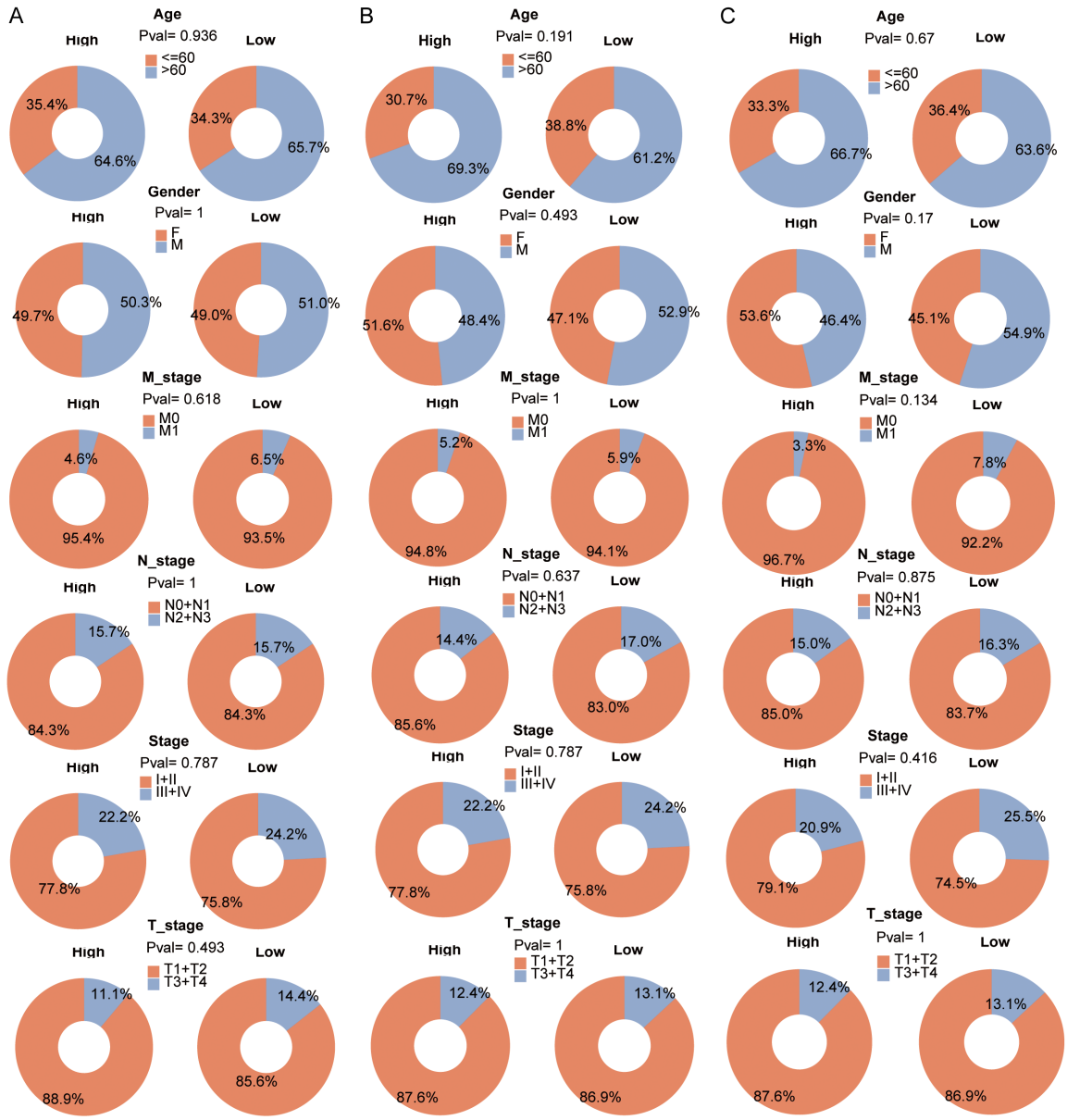

Figure S2. Association of ETVs expression with clinicopathological features. (A-C) Donut charts depicting the distribution of age, gender, M stage, N stage, T stage, and overall stage in patients stratified by high versus low mean methylation of significant ETV1 (A), ETV4 (B), and ETV5 (C) sites.

ETV5 upregulates FOXA2 in LUAD

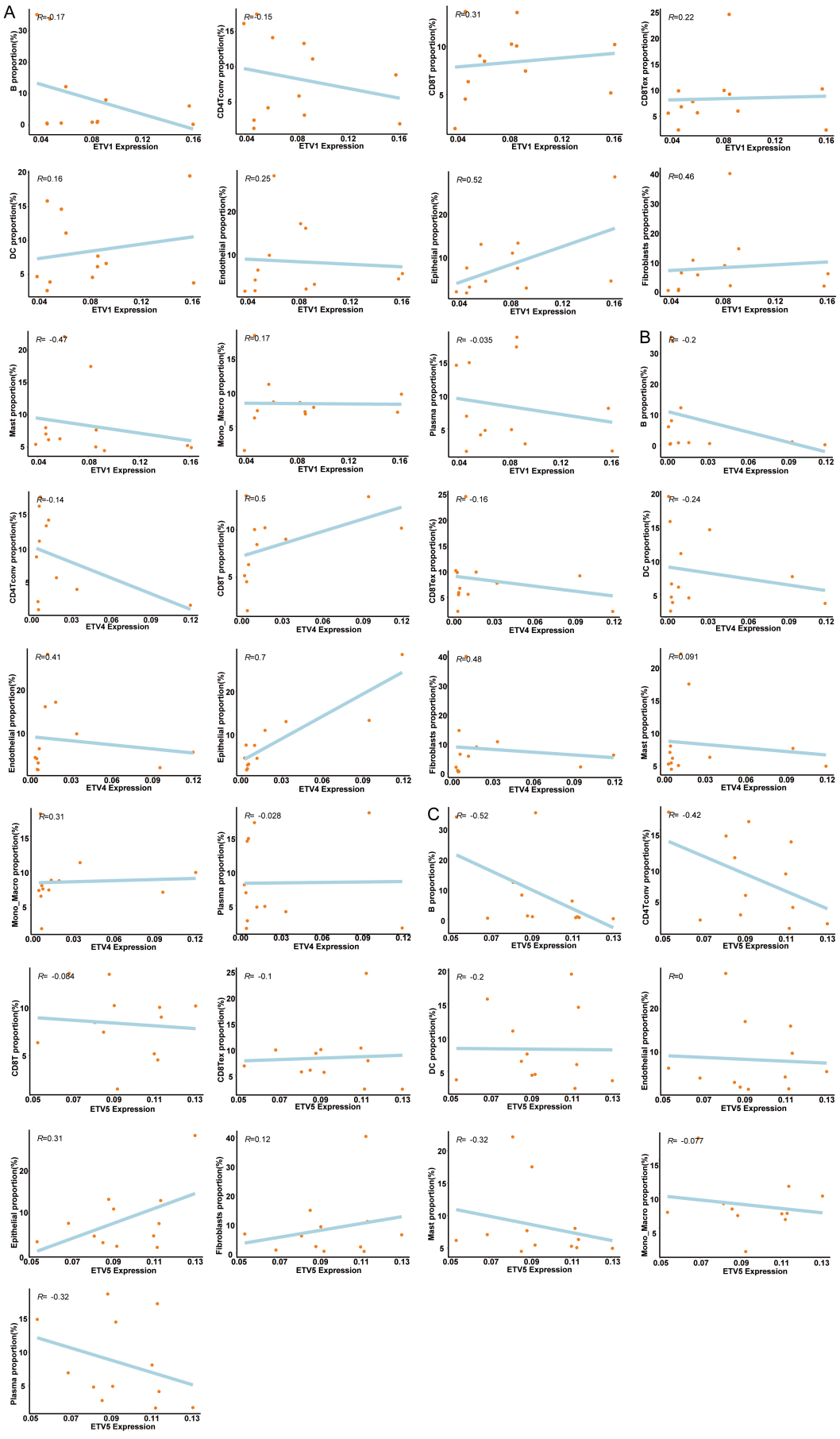

Figure S3. Association between ETV1/ETV4/ETV5 expression levels and the proportions of distinct cell types in the tumor microenvironment. (A-C) Pearson correlation analysis between ETV1 (A), ETV4 (B), and ETV5 (C) expression and the proportions of the indicated cell types in the GSE131907 scRNA-seq dataset (11 tumor and 11 matched normal samples).

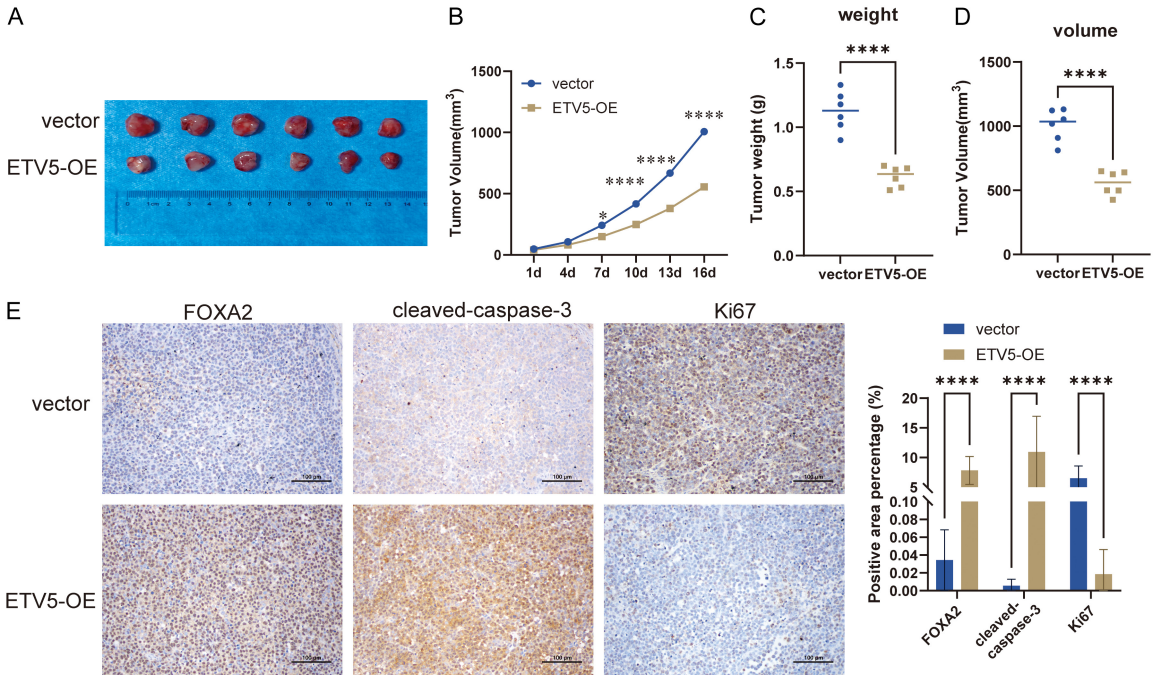

Figure S4. ETV5 overexpression suppresses LUAD tumor growth *in vivo*. A. Representative images of subcutaneous xenograft tumors derived from A549 cells stably expressing the control vector or ETV5-overexpression construct. B. Tumor growth curves exhibiting changes in tumor volume during the indicated observation period. C. Tumor weights measured at the experimental endpoint. D. Final tumor volumes in vector and ETV5-OE groups. E. Representative immunohistochemical staining and quantitative analysis of FOXA2, caspase-3, and Ki67 expressions in the xenograft tumor tissues. Magnification, 200×; Scale bar, 100 μm. $^{*}P < 0.05$, $^{****}P < 0.0001$.